Technical note: An assessment of the performance of statistical bias correction techniques for global chemistry-climate model surface ozone fields

Christoph Staehle[1], Harald E. Rieder[1], Arlene M. Fiore[2], Jordan L. Schnell[3,4]

[1]Institute of Meteorology and Climatology, BOKU University, Vienna, Austria

[2]Department of Earth, Atmospheric and Planetary Sciences, Massachusetts Institute of Technology, Cambridge, MA, USA

[3]Cooperative Institute for Research in Environmental Sciences, University of Colorado Boulder, CO, USA

[4] NOAA Global Systems Laboratory, Boulder, CO, USA

Correspondence to: christoph.staehle@boku.ac.at

Abstract. State of the art chemistry-climate models (CCMs) still show biases compared to ground-level ozone observations, illustrating remaining difficulties and challenges in the simulation of atmospheric processes governing ozone production and loss. Therefore, CCM output is frequently bias-corrected in studies seeking to explore the health or environmental impacts from changing air quality burdens and associated impacts. Here we assess four statistical bias correction techniques of varying complexity, and their application to surface ozone fields simulated withinof four CCMs, and evaluate their performance against gridded observations in the EU and US. For the evaluation of the raw CCM outputs and the performance of the individual adjustment techniques Wwe focus on two time periods (2005-2009 & 2010-2014), where the first period is used for development and training and the second to evaluate the performance of techniques when applied to model projections. Our results showWe find, that while all methods applied are capable of significantly reducing the model bias.,However, but better results are biases are lowest obtained when we applyfor more complex approaches such as quantile-mapping and delta-functions. We also highlight the sensitivity of the correction techniques to individual CCM skill at reproducing the observed distributional change in surface ozone. Ensemble simulations available for one CCM indicate thate model ozone biases arises are likely more likely from sensitivitiessensitive to the process representation embedded in chemical mechanisms or emissions rather than todriving meteorology.

1 Introduction

Surface ozone (O_3) is both an air pollutant and greenhouse gas, formed in photochemical reactions involving precursor substances such as nitrogen oxides (NO_x) and volatile organic compounds (VOCs) of both anthropogenic and non-anthropogenic origin [e.g. Checa-Garcia et al., 2018; Lelieveld & Dentener, 2000; Monks et al., 2015]. In addition to the availability of precursor gasses, the NO_x to VOC ratio as well as solar radiation and ambient air temperature, controlling emissions of biogenic VOCs (BVOCs) and chemical reaction rates, play a crucial role for O_3 formation [Chameides et al., 1988; Sillman, 1999; Sillman et al., 1990]. Tropospheric O_3 abundance is also substantially influenced by stratospheric intrusions [Stohl et al., 2003], which can, in certain regions [Lin et al., 2015] or during specific events, [Akritidis et al., 2010] alter concentrations significantly [Akritidis et al., 2010; Lin et al., 2015; Stohl et al., 2003]. O_3 is associated with a variety of detrimental human health effects, especially in the context of the respiratory and cardiovascular system, resulting in about 5-20 % of premature deaths attributable to ambient air pollution [Gu et al., 2023; Malashock et al., 2022; Monks et

al., 2015; Murray et al., 2020; Pozzer et al., 2023; Zhang et al., 2019]. In addition to its negative health effects, O_3 ~~is considered to~~can compromise the metabolism of plants through stomatal uptake and ~~to~~ cause damage to leaf surfaces, thereby affecting biomass and crop production [Da et al., 2022; EEA, 2020; Fleming et al., 2018; Mills et al., 2018; Monks et al., 2015]. Consequently, a large body of studies examine past, present and future development of surface O_3 burdens as well as resulting health and ecological impacts on both regional and global scale [e.g. Da et al., 2022; Meehl et al., 2018; Nolte et al., 2018; Westervelt et al., 2019].

Studies ~~seeking to~~ explor~~ing e~~ing future changes in surface O_3 burdens and their implications for human health and the biosphere rely on ~~outputs~~ simulated fields of chemistry-climate models (CCMs) and chemistry-transport models (CTMs). However, despite ongoing development, these models show deficiencies in the adequate representation of ~~tropospheric~~ ground-level O_3 on regional to local scale and changes therein when ~~. Especially global scale models are known to be biased~~ compared to observations [e.g. Griffiths et al., 2021; Karlický et al., 2024; Turnock et al., 2020; Young et al., 2018]. This shortcoming~~,~~ rais~~ing the~~esing questions regarding the reliability of the simulated surface ozone response to changes in precursors and ambient climate. The number of possible reasons for the deviation of model output and observations ~~is basically~~ increas~~ing~~esing with the complexity of the models. However, the published literature commonly suggests issues with emissions fed into the models, the applied chemical mechanism, meteorology ~~or~~ and deposition in addition to uncertainties associated with the spatial resolution [e.g. Archibald et al., 2020; Liu et al., 2022; Young et al., 2018]. To overcome th~~is~~ese issue~~s~~, also as individual experiments are computationally expensive similar to climate studies, statistical bias correction techniques of different complexity are frequently applied to correct global model fields. Such corrections allow the diagnosis of changes in ambient meteorological conditions and ozone in isolation or combination and to investigate related impacts on human health. Machine learning approaches are increasingly being used for correction purposes [e.g. Liu et al., 2022]. These methods, however, usually have the disadvantage of behaving like a "black box", i.e. algorithms lack traceability and thus physical insights as to the root cause of biases. To date no detailed comparison of different statistical bias correction techniques for surface ozone burdens has been performed and the present study aims to close this gap.

Here we analyze historical simulations from 3 different global CCMs contributing to the Coupled Model Intercomparison Project phase 6 (CMIP6), as well as a 13-member ensemble of the CESM2-WACCM6 model for the European (EU) and contiguous United States of America (US) domain. For an assessment of model performance, we compare model outputs with gridded observational datasets available for both domains. First, we evaluate the ozone fields of the individual CCMs with observations and contrast the magnitude, sign and seasonality of the bias among CCMs. Thereafter, we apply a set of statistical bias correction techniques aiming for a reduction of the initial bias, independent of its origin, and evaluate the performance of these methods to identify if a particular correction technique is preferable across models.

Since the model simulations are "free-running", and thus create their own meteorology internally, a direct day-to-day comparison with the observations is not meaningful. Hence, our analysis primarily aims to evaluate the distribution of the O_3 fields in a statistical sense. Given the importance of ozone for human health we focus on the upper tail of the maximum daily 8-hour average (MDA8) O_3 distribution, and the frequency of occurrence of exceedance of health-related target values for Europe and the US.

2 Data & Methods

2.1 Model and observational data

75 The O_3 data sets explored in our analysis are hourly surface O_3 outputs from three CCMs (GFDL-ESM4, UKESM1-0-LL and EC-Earth3) contributing to CMIP6, and a 13-member ensemble simulation created with CESM2-WACCM6. For most of our study, we use only the first ensemble member of CESM2-WACCM6 ~~(notewe use for the bulk of the present study only the first ensemble member, we do so~~ in analogy to the other CCMs, given the overall heterogeneity in the number of members ~~per model~~ available per model. In section ~~4.3~~3.4, we focus on~~ing~~ the chemical vs. meteorological driving of model

80 biases and~~, we~~ utilize the entire CESM2-WACCM6 ensemble ~~available.~~ ~~is used for the main part of this study), from which we calculate maximum daily eight-hour average (MDA8) O_3 values~~.

We also obtain observed MDA8 O_3 with a spatial resolution of 1° x 1° per grid cell for both the European and the US domain using an extended dataset constructed using the methods of Schnell et al. [2014]; [2015]~~Schnell et al. [2014; 2015]~~ and Schnell and Prather [2017]~~Schnell and Prather [2017]~~, one which was designed specifically to compare against gridded

85 CCMs. The dataset is constructed using an inverse distance weighted interpolation method that includes a declustering component similar to kriging; i.e., clustered (within 100 km) observations' weights are reduced such that those stations (often located around urban centers) are not disproportionately used in the interpolation. For the US domain, point based observations that are used in the interpolation include the US EPA's Air Quality System (AQS), the US EPA Clean Air Status and Trends Network (CASTNET), and Environment Canada's National Air Pollution Surveillance Program (NAPS);

90 for the European Domain we include the EMEP and European Environment Agency's AirBase network (excluding stations designated as traffic). The exponent for the distance component is 2.5 and a maximum distance of 500 km is used for the weights. Parameters were estimated using a leave-N-out cross-validation technique. Estimations are made at 25 equally spaced points within each 1° x 1° cell and trapezoidally averaged. ~~The interpolation is performed on hourly abundances and the MDA8 O3 is estimated using the interpolated hourly fields.~~ Other recent work has used this extended dataset [e.g.,

95 Ducker et al., 2018; Garrido-Perez et al., 2019; Guo et al., 2018]~~(e.g., Ducker et al., 2018; Garrido-Perez et al., 2019, Guo et al., 2018)~~. Schnell et al. [2014]~~Schnell et al. [2014]~~ estimated an RMSE of 6-9 ppb for individual stations and 0-3 ppb for the grid cell averages; Ducker et al. [2018]~~Ducker et al. [2018]~~ estimated a mean bias of 5-10 ppb with the updated dataset over their study locations. For the analysis here the interpolation is performed on hourly abundances and the MDA8 O_3 is estimated using the interpolated hourly fields. Note, we apply the nomenclature of the European Union for the calculation of

100 the MDA8 O_3 values in both domains, i.e. the eight hour average for a given hour is derived using the data of that specific hour and the preceding seven hours [EUR-LEX, 2008]. For convenience, the data is provided on a public repository, see data statement below. ~~DISCUSS OBS DATA in detail!~~

~~We also use observational MDA8 O3 data derived from gridded hourly datasets, with a spatial resolution of 1° x 1° per grid cell and a~~ REWRITE SECTION for REVISED ~~manuscript temporal extent of 1993 to 2014 for both the European and the~~

105 ~~US domain [Schnell et al., 2014].~~

To allow for an optimal comparison, the model data is regridded using an ordinary inverse distance weighting algorithm to match the spatial extent of the observations. In addition, all data sets are harmonized regarding their temporal resolution by removal of days not included in any of the other datasets, resulting in a 358-day calendar (30 days per month except for February). MDA8 O_3 is derived for each dataset and time step according to the European nomenclature as mentioned above.

110 For the historical analysis we use 2005 to 2009 to evaluate the baseline bias of the individual CCMs and establish the

performance of individual bias correction techniques. The time slice 2010 to 2014 is used subsequently, to evaluate the performance of our methods for model projections.

2.2 Bias correction methods

For statistical bias correction we apply four different techniques, which are detailed below. Here M_q and O_q denote quantiles ($q \in 1, ..., N \mid 1 = min, N = max$) of the model and observational distributions, respectively. The running index j marks individual MDA8 O_3 model values. Additionally, we use the indices $hist$ and $proj$ to differentiate between historical and projected data. Primed terms indicate the bias corrected model outputs.

2.2.1 Mean bias correction (MB)

$$\overline{\Delta M} = \frac{1}{N} \sum \left(M_q^{hist} - O_q^{hist} \right) \tag{1}$$
$$= \overline{M_q^{hist}} - \overline{O_q^{hist}}$$
$$M_q'^{proj} = M_q^{proj} - \overline{\Delta M} \; ; \; M_q'^{hist} = M_q^{hist} - \overline{\Delta M} \tag{2}$$

The MB is a commonly used approach assuming a constant offset between model and observations. ̶As an initial step we derive the average difference of the historical model and observational percentiles (alternatively the difference between the mean values of both empirical cumulative distribution functions (ECDFs) can be computed). Subsequently we subtract the result of Eq. (1) from each quantile of the projected model distribution to retrieve a bias corrected model ECDF (Eq. (2)).

2.2.2 Relative bias correction (RB)

$$\bar{c} = \frac{1}{N} \sum \left(\frac{M_q^{hist} - O_q^{hist}}{O_q^{hist}} \right) \tag{3}$$
$$M_q'^{proj} = M_q^{proj} - \bar{c} * O_q^{hist} \tag{4}$$

Here, similar to the MB method, we assume that model and observations differ by a constant factor. In contrast to the MB correction, however, we derive the average of the relative deviation of the historic model and observational percentiles (Eq. (3)). The bias corrected model projection (Eq. (4)) is then calculated as the difference between the raw model and the observed quantiles times the correction term established in Eq. (3).

2.2.3 Delta correction (DC)

$$\Delta M_q = M_q^{proj} - M_q^{hist} \tag{5}$$
$$M_q'^{proj} = O_q^{hist} + \Delta M_q \tag{6}$$

The DC approach follows the methodology detailed in Rieder et al. [2018]. In contrast to the MB and RB~~DC~~ methods it is assumed that, while the individual model values may be biased, the system response (i.e., change between two time periods) is represented adequately by the model. Therefore the deviation between future and base period model data is calculated for all quantiles individually (Eq. (5)). Finally the corrected model projection is derived as the observed distribution plus the initially computed model change (Eq. (6)).

2.2.4 Quantile mapping (QM)

$$R_q^{hist} = \frac{O_{q+1}^{hist} - O_q^{hist}}{M_{q+1}^{hist} - M_q^{hist}} \tag{7}$$

$$c_j^{hist} = R_q^{hist} * \left(M_j - M_q\right); \; M_q \leq M_j < M_{q+1} \tag{8}$$

$$M_j'^{hist} = O_q^{hist} + c_j^{hist} \tag{9}$$

$$\Delta M_q = M_q^{proj} - M_q^{hist} \tag{10}$$

$$m_q'^{proj} = M_q'^{hist} + \Delta M_q \tag{11}$$

$$R_q^{proj} = \frac{m_{q+1}'^{proj} - m_q'^{proj}}{M_{q+1}^{proj} - M_q^{proj}} \tag{12}$$

$$c_j^{fut} = R_q^{proj} * \left(M_j^{proj} - M_q^{proj}\right); \; M_q^{proj} \leq M_j^{proj} < M_{q+1}^{proj} \tag{13}$$

$$M_j'^{proj} = m_q'^{proj} + c_j^{proj} \tag{14}$$

The term "quantile mapping" summarizes a variety of similar bias correction approaches used within the climate research community [e.g. Lehner et al., 2023]. Here, however, we follow the method described for CCM outputs in Rieder et al. [2015]. In contrast to the other methods used in this study, the QM is a multi-step approach. The first steps, illustrated in Eq. (7) to (9), consist of the computation of a bias corrected historic model distribution. Next, the result is used to create a ~~distribution of a~~ bias corrected future ECDF, similar to the DC method (Eq. (10) and (11)), which is then employed to derive the bias corrected future model data (Eq. (12) to (14)). In contrast to Rieder et al. [2015] however, who suggested a fixed apportionment for the quantiles ~~used~~ to avoid non-~~ ~~meaningful results by executing ~~not~~ undefined operations, especially in Eq. (7) and (12), (i.e. denominator equals zero or both denominator and numerator equal zero), we employ here a variable algorithm to select~~ing~~ the optimal ~~amount~~ number of percentiles for each individual realization of the QM method~~ individually~~. This is achieved by fixing the minimum and maximum values of the model ECDF and allowing for all quantiles with unique values within this range, i.e., if several quantiles share the same value, which might be the case, especially for narrow distributions, only the first quantile is used.

All four methods are applied to the ECDFs of the individual CCM datasets (1) on a monthly basis within the base time interval, (2) for each grid cell individually (in contrast to Rieder et al. [2015], who used a regional approach), (3) for both the EU and US domains. While it is implied that the model data differs from the observations by a constant factor for the MB and RB methods, the DC and QM techniques assume that the difference between the future and reference period is represented adequately in the individual models, independent of the prevailing model bias. In contrast to the QM method, which provides the opportunity to directly correct individual daily MDA8 O_3 values, the application of the MB, RB (according to the methodology detailed above) and DC techniques solely results in new model ECDFs. The mapping algorithm, detailed in Eq. (7) to (9) is therefore applied further to the outputs of these three correction methods. Thereby the model data is mapped onto the bias corrected ECDFs, allowing for an optimal comparison of original- and bias corrected model data with the observations and the results from the other correction techniques under investigation here.

180 To quantify the initial biases as well as the remaining bias after application of the individual correction techniques we derive the number of days above the target value for the protection of human health (120 μg/m^3 in the EU (approximately 60 ppb) and 70 ppb in the US) and the residual bias of the ECDFs on seasonal and annual time scales [EPA, 2015; EUR-LEX, 2008, 2011].

3 Results

185 **3.1 Model evaluation**

We start by evaluating the performance of the global models in representing the MDA8 O$_3$ burden for the historical time period (2005-2009). Fig. 1a,b shows the pooled MDA8 O$_3$ probability density function for models and gridded observations for the EU and US domains. Pronounced differences emerge between the individual models and observations for both domains. Generally, the models are biased high compared to observations, and the amplitude of the bias varies substantially

190 among models. One exception in this regard is the EC-Earth3 model, which shows a high bias compared to observations across the majority of the MDA8 O$_3$ distribution but in contrast to other models a low bias at the upper tail.

We further investigate the magnitude of the model biases in Fig. 1c,d by contrasting the annual average number (and seasonal partitioning) of days above the target value to protect human health, defined as 60 and 70 ppb for the EU and US domains, respectively. For the observations we find a domain average number of exceedance days of the target values of 8

195 (five for summer and 3 for spring) and 3 (2 for summer and 1 for spring) days for the EU and US domains in 2005-2009. While the models agree with observations regarding a preferred occurrence of non-attainment days in summer season, all models but EC-Earth3 substantially overestimate the occurrence frequency of exceedance days. The domain average bias in non-attainment days for the EU ranges between 5 days in EC-Earth3 and 113 days in UKESM1-0-LL. In contrast, values for the US vary between 2 to 79 days. Overall our findings indicate a slightly better agreement of CCMs regarding the policy

200 relevant metrics in the US than EU, which has to be taken with caution given also the regional difference in the MDA8 O$_3$ target value. Assuming the same target threshold as for Europe, we find that the number of exceedance days ranges between 20 and 174. Table 1 provides a summary of the occurrence frequency of MDA8 O$_3$ extremes for models and observations on an annual and seasonal basis (note, fall and winter are grouped together (FW) due to the small number of exceedance exceedance days derived for these seasons).

205

			2005-2009		
	Obs	**EC-Earth3**	**CESM2-WACCM6**	**GFDL-ESM4**	**UKESM1-0-LL**
MAM	3 (1; 7)	1 (0; 4)	4 (2; 17)	4 (2; 10)	43 (18; 63)
JJA	5 (2; 12)	4 (2; 12)	13 (10; 29)	27 (18; 42)	57 (51; 78)
FW	0 (0; 2)	0 (0; 4)	1 (1; 5)	4 (2; 8)	13 (10; 33)
annual	8 (3; 21)	5 (2; 20)	18 (13; 51)	35 (22; 60)	113 (79; 174)
			2010-2014		
MAM	1 (0; 5)	0 (0; 2)	3 (1; 15)	2 (1; 6)	39 (10; 58)
JJA	3 (1; 8)	1 (1; 6)	9 (7; 24)	29 (17; 40)	54 (37; 72)
FW	0 (0; 2)	0 (0; 2)	1 (1; 6)	4 (1; 8)	14 (6; 27)
annual	4 (1; 15)	1 (1; 10)	13 (9; 45)	35 (19; 54)	107 (53; 157)

Table 1: Average number of exeedance days (i.e., the number of days above the target threshold of 60 ppb (EU) and 70 ppb (US), respectively) per grid cell derived from observations and individual raw model data for the EU and US (given in parenthesis) for ~~summer (JJA),~~ spring (MAM), summer (JJA), fall and winter (FW) and annual. Note numbers in italics in the parentheses are derived applying the EU threshold for the US.

Next, we turn to model biases in the spatial domain. Figure 2 shows the difference in the average number of days above the target value for individual models to observations (note, grey shaded areas indicate a marginal difference of up to ± two days). The spatial distribution of differences confirms the biases detailed above, showing regionally varying but distinct biases of the models examined. Of the models examined, the EC-Earth3 model performs best in both domains with a domain average bias of +7 (EU) and +3 days (US), respectively. While pronounced differences in the magnitude of the bias between individual models occur, the spatial patterns in bias ~~occurrence~~ are quite similar. In particular a north to south gradient emerges in the European domain with significantly higher model biases in the Mediterranean region and small to negligible biases in Scandinavia and the UK. For the US we find across models less pronounced biases in the Midwest, while substantial biases emerge in the North- and Southeast ~~t~~and Southwest.

To investigate the consistency of the spatial bias in models compared to observations we expand the analysis to the 2010-2014 time period (Fig. S1 & S2). Although slight variations are found for individual seasons, overall the result for this time period resembles those obtained for 2005-2009 in both the US and EU domain (see Fig. S1). This result provides further confidence in the robustness of our assessment of general model biases in the MDA8 O_3 distribution and the modelled frequency of non-attainment days.
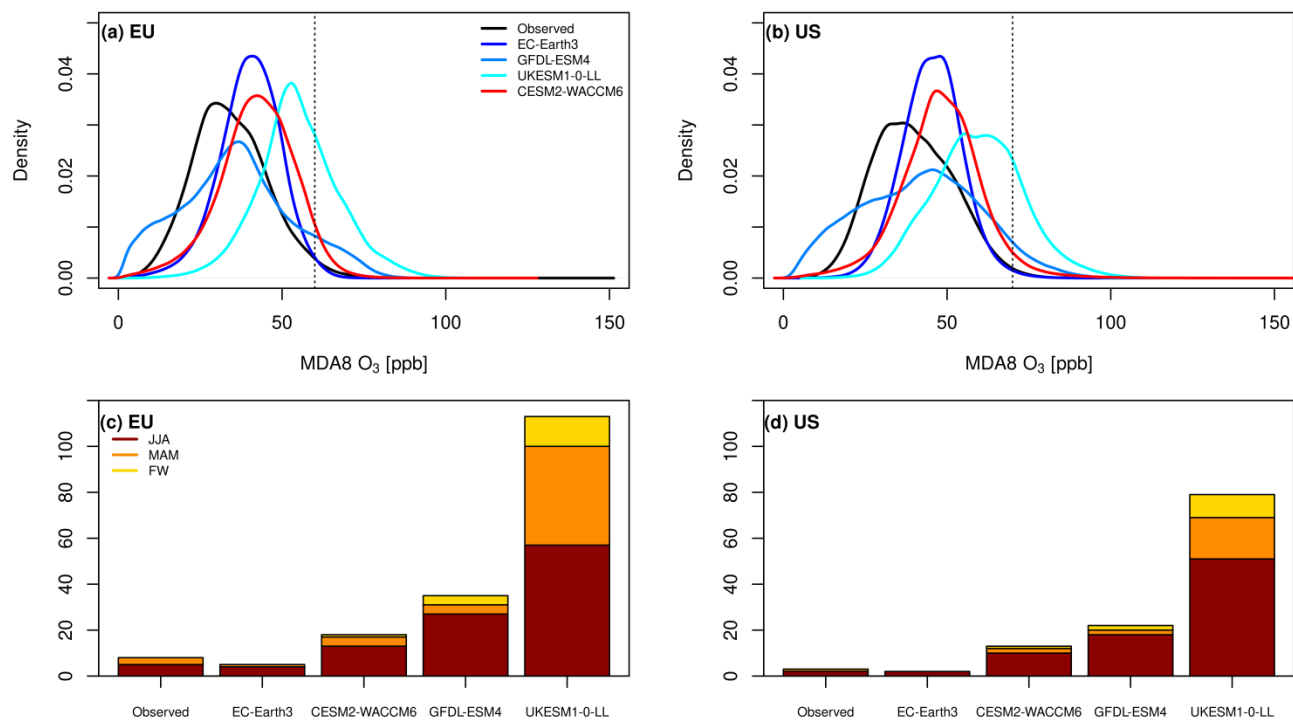
Fig. 1: Probability density function (PDF) of observed (black) and modeled (coloured) MDA8 O_3 during 2005 to 2009 in the EU (a) and US (b) domain. Average number of days above the MDA8 O_3 target value per grid cell for summer (JJA –

red), spring (MAM – orange) as well as fall and winter months (FW – yellow) during 2005 to 2009 in the EU (c) and US (d) domains. In panels (a) and (b) dashed vertical lines indicate the target value for the protection of human health. The annual average number of exceedance days in (c) to (d) is given by the sum of the individual segments, i.e. the total height of the bars.
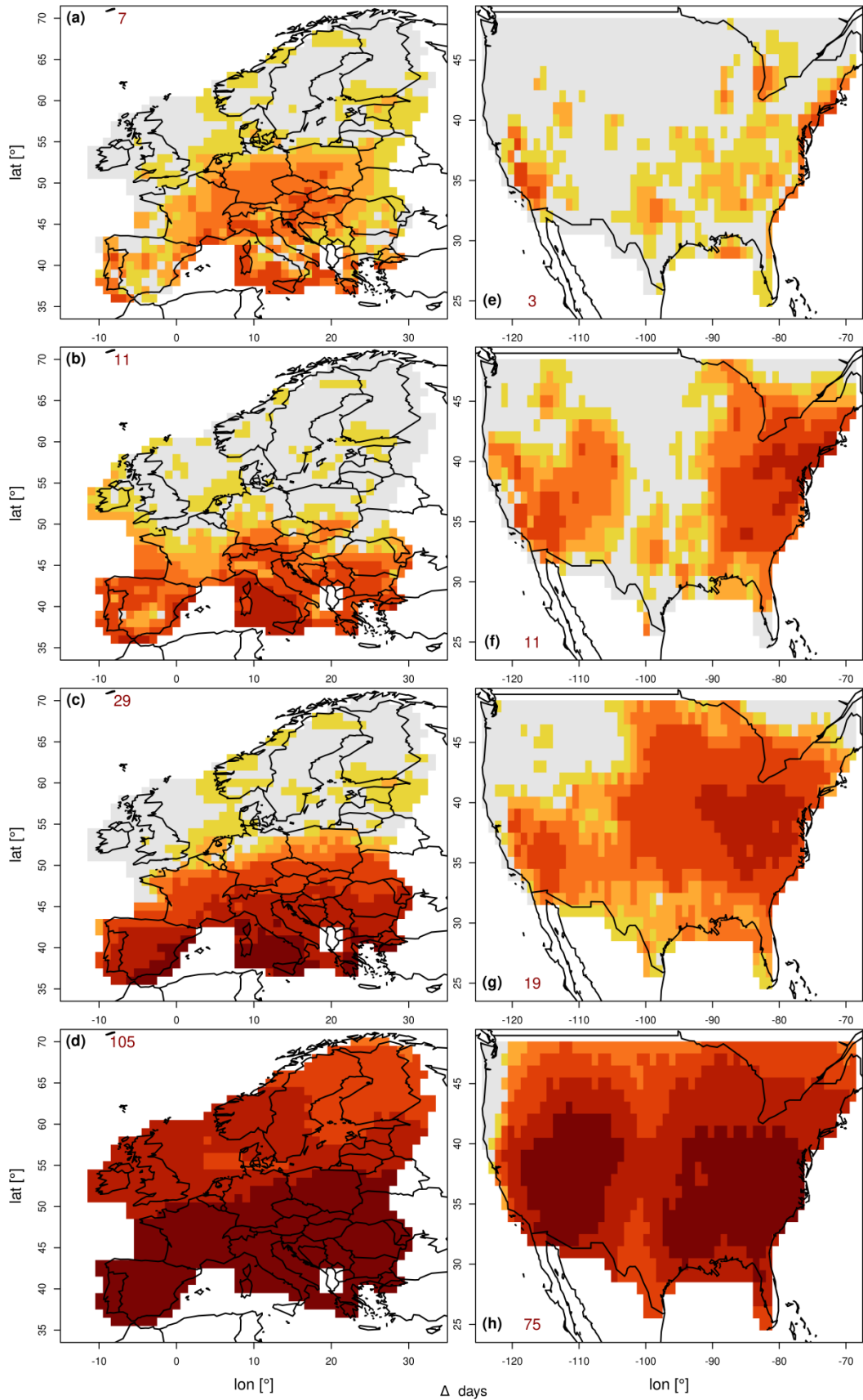
Fig. 2: Difference in the average number of days above the MDA8 O_3 target value in CCM simulations (EC-Earth3 a & e, CESM2-WACCM6 b & f, GFDL-ESM4 c & g, UKESM1-0-LL d & h) compared to gridded observations for the European (left) and US domain (right). All panels show~~for~~ differences during 2005-2009. Red numbers in the upper/lower left corner indicate the grid cell average anomaly. Grey shading indicates differences within $\pm$ 2 exceedance days.

3.2 Bias correction for the base period 2005-2009

Having illustrated the model biases for the past, we turn next to bias correction. To this end we apply the individual bias correction methods to model outputs for 2005-2009 and evaluate their performance for the MDA8O_3 distribution and the number of non-attainment days. The DC method represents an exception in this case as applying this method, by definition, would yield a "perfect" agreement with the observational ECDF. Accordingly, any potential deviations from observed ECDF would be a mere result of uncertainties associated with implementation, in particular the mapping algorithm and rounding, and thereby do not represent the performance of the DC method in context of the base dataset. The performance of the DC method will be however, assessed, along with the other methods when applied to the evaluation period 2010-2014.

Figure 3 shows the distribution of the grid-cell level bias in the number of ~~exeedance~~exceedance days for the European (a – d) and US (e – h) domains. All methods ~~applied~~ reduce the bias substantially. The MB and RB methods yield similar results. Both methods tend to overcorrect the bias, yielding residual biases for individual grid-cells varying between -22 and +8 days (EU) and -10 to +6 days (US), with MB performing slightly better. In contrast, the QM method yields an almost perfect agreement (comparable to the DC method as detailed above) with observations. Residual biases are between -2 and +1 days for Europe and 0 days for the US.

Spatial distributions of the anomaly on ~~exeedance~~exceedance days~~,~~ are illustrated in Fig. S3 and S4. We find that the application of a particular method yields similar spatial patterns of improvement independent of the model to which it is applied and of the initial model bias. For the MB and RB approaches, the spatial gradient in the bias identified in the raw models remains for the EU domain, although with reversed sign for the majority of applications, i.e.~~,~~. stronger overcorrection in the Central Europe and the Mediterranean than in the northern parts of EU domain. For the US the MB and RB methods perform better compared to Europe. This finding, however, is attributable to the higher target threshold rather than the actual performance of these methods as shown in section 3.1. The QM method ~~corrected outputs agree~~ best captures ~~with~~ the observations in both domains.

We examine the PDFs of the bias~~-~~-corrected model data for conformity with the observations (see Fig. S5). While all correction methods lower the bias across the whole distribution, the MB and RB approaches~~,~~ still deviate from the observations. In contrast, the distribution of the QM-corrected data is almost perfectly aligned with the observational PDF, independent of the model and domain. In summary, our evaluation for the baseline period indicates a clear preference for the QM (or the DC) method.
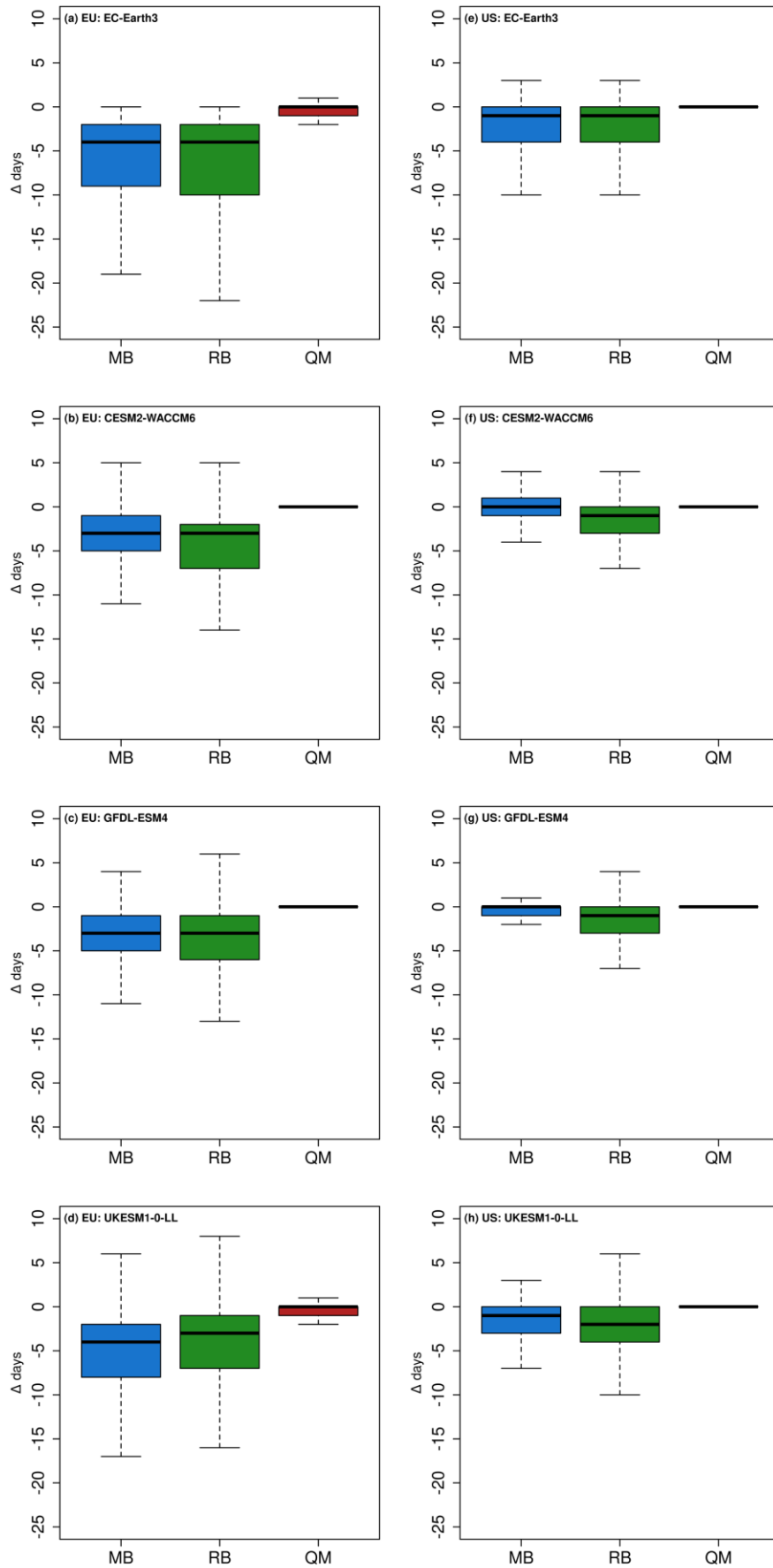
Fig. 3: Boxplots of the average residual bias in exceedance days pooled across grid cells in the individual CCMs in 2005-2009: (a) EC-Earth3, (b) CESM2-WACCM6, (c) GFDL-ESM4 and (d) UKESM1-0-LL models in the EU domain, (e) ,(f),(g),(h) as (a) ,(b),(c),(d) but for the US domain. Blue, Green and red colour indicate the MB, RB and QM correction methods respectively.

3.3 Bias correction performance in the evaluation period 2010-2014

Next, we turn the focus to the results obtained with individual bias correction techniques during the evaluation time period (2010-2014). We apply the adjustment methods to the MDA8 O_3 outputs of the individual models, but treat the data as independent realizations, in order to assess the methods performance for their applicability to future projections (see section 2).

Figure 4 shows the distribution of the residual grid-cell level mean bias compared to observations for the number of exceedance days of the target value. Here we find a larger residual bias, ranging between -17 and +11 exceedance days in the European domain (Fig. 4a-d) than in the US (Fig. 4e-h) where the bias after correction varies at grid level between -5 to +5 days across grid cells. Furthermore, contrasting the performance of the individual bias correction techniques yields a curious result, as we no longer identify an individual correction technique as optimal across models and spatial domains.

We further explore the spatial distribution of the residual bias. Compared to the base period the MB and RB (see Fig. S6-S7 a-d & e-h) corrected models show an improved agreement compared to observations. While the spatial patterns of bias distributions are similar to the 2005-2009 period (except for the GFDL-ESM4 model) an improvement compared to the base period is found for the northern and eastern European countries as well as the south-east US. The residual bias worsens in the central EU and the Mediterranean as well as the south-west US when applied to the GFDL-ESM4 model. For the DC and QM approaches (see Fig. S6-S7 i-l & m-p) on the other hand, we find a significantly increased residual bias (of both positive and negative sign), independent of model and domain.

Although all methods applied are still capable of significantly reducing the bias, these results, in contrast to those for the base period, no longer allow the identification of a sole ideal correction method, indicating changes in the underlying processes contributing to the bias. Our findings show that the correction approach yielding the lowest residual bias varies strongly across models and spatial domain. For example, while the QM method performs best for the CESM2-WACCM6 in the EU domain (Fig. 4b) the RB method yields a smaller residual bias in the US (Fig. 4f).

These results are supported by the analysis of the PDFs of the bias corrected model output (Fig. S8). While the conformity with observations remains widely similar for the majority of the distribution, the adjustment of the high tail yields slightly better results in context of the MB and RB methods, when compared to the base period. Contrarily, the distributions of both the DC and QM methods show a good agreement with the low tail and the midsection of the observational PDF. The performance however, is deteriorates ing towards the high tail, partially resulting in an overestimation of the monitored distribution, especially in the European domain.

To further investigate this curious result we examine, on a quantile basis across the MDA8 O_3 distributions, i) the error resulting from the initial bias correction of the base period (E_B) and ii) the error resulting from the deviation of the models change between the base and evaluation period when compared to observations (E_Δ).

$$E_B = M_q'^{hist} - O_q^{hist} \tag{15}$$

$$E_F = M_q'^{proj} - O_q^{proj} \tag{16}$$

$$= \left(M_q'^{hist} + \Delta M_q \right) - \left(O_q^{hist} + \Delta O_q \right)$$
$$= E_B + \Delta M_q - \Delta O_q = E_B + E_\Delta$$

The results of this analysis are exemplarily shown for the CESM2-WACCM6 model in Fig. 5 for the EU (a-c) and the US (d-f) (note the illustrations for the other models are included in the supplemental Fig. S9-S10). Here the red shading indicates the minimum to maximum range of the residual bias across grid cells for the base period after bias correction (E_B, Eq. (15)), and the solid red line shows the domain average of this bias at individual quantiles concerned. In contrast the grey shading illustrates the minimum to maximum range of the differences in the change between the base and evaluation period of the raw model and observations, respectively (E_Δ, Eq. (16)). The black solid line marks the domain average of this bias at individual quantiles concerned. The residual bias for the evaluation period E_F (or in analogy any other future time period) comprises the sum of these errors (base bias and response bias) and is illustrated for the domain average with the dashed yellow line. We note that, as the DC method by definition yields no initial error in the base period only E_Δ is relevant in the evaluation period which is illustrated by the grey shading and the black solid line in all panels of Fig. 5 (as well as Fig. S9-S10).

For the base period it is apparent that the QM correction technique, in contrast to RB and MB correction, yields only minor differences across the MDA8 O_3 distribution when compared to the observations in both spatial domains. For the evaluation period we see that the difference in response between models and observations is dominating over the raw performance of the individual correction techniques and that the residual bias depends strongly on region and model concerned (see Fig. 4-5 and supplemental Fig. S9-S10). Given this result, we assume This illustratesthat the dependence of correction performance depends strongly on models being able to represent precursor emission changes over time as seen in observations.

All models show distinct biases in reproducing observed ozone changes between the two time periods, with ain magnitude particularly pronounced magnitude in the tails of the distributions. Although both error terms, and the resulting net error are found to be rather small in the domain average (roughly ±5 ppb), they might have a strong influence on the individual grid cell level (see shadings). Especially for the MB and RB techniques the individual errors might compensate each other, as illustrated by the improved results relative to the base period. The DC and QM approaches on the other hand strongly depend on the quality of the model response in time. Here we find, that pronounced errors in the model change offset (at least in parts) the benefits illustrated for the base period (see Fig. 4).
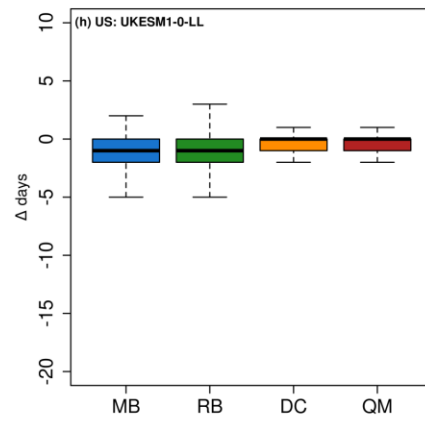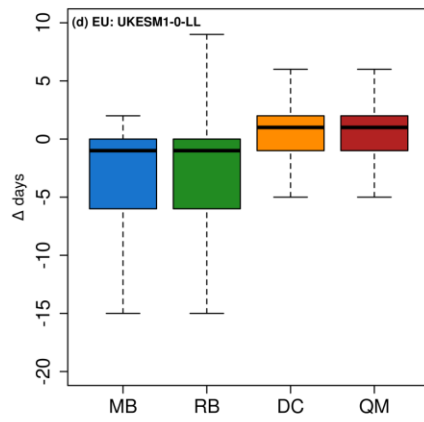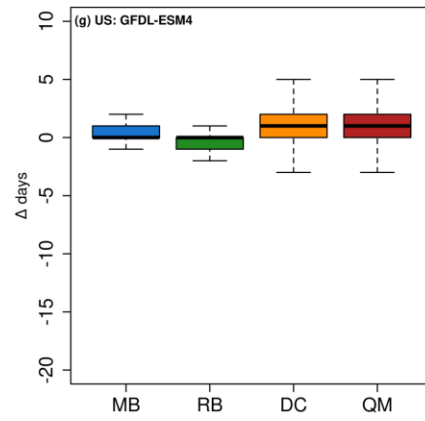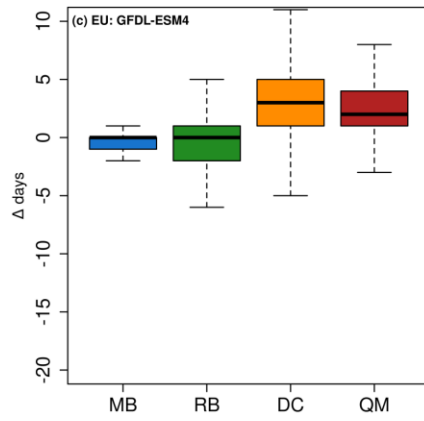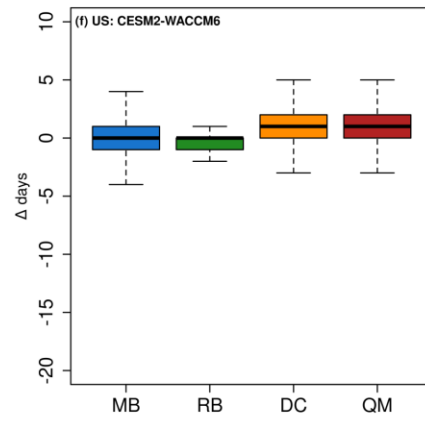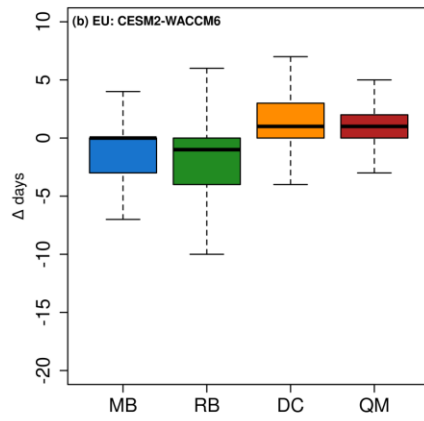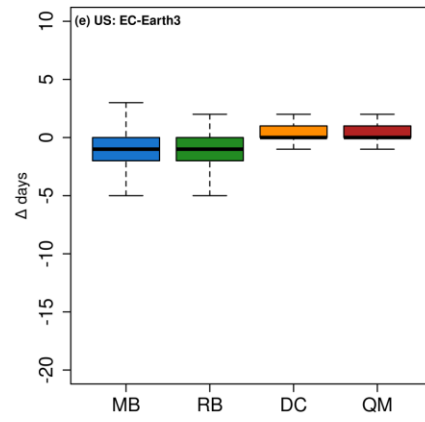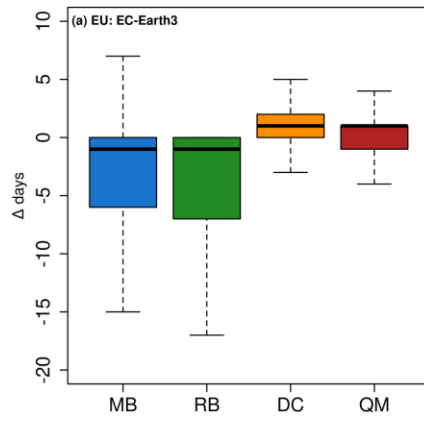
Fig 4: As Fig. 3 but for 2010-2014 time period. Blue, Green, orange and red colour indicates the MB, RB, DC and QM correction methods respectively.
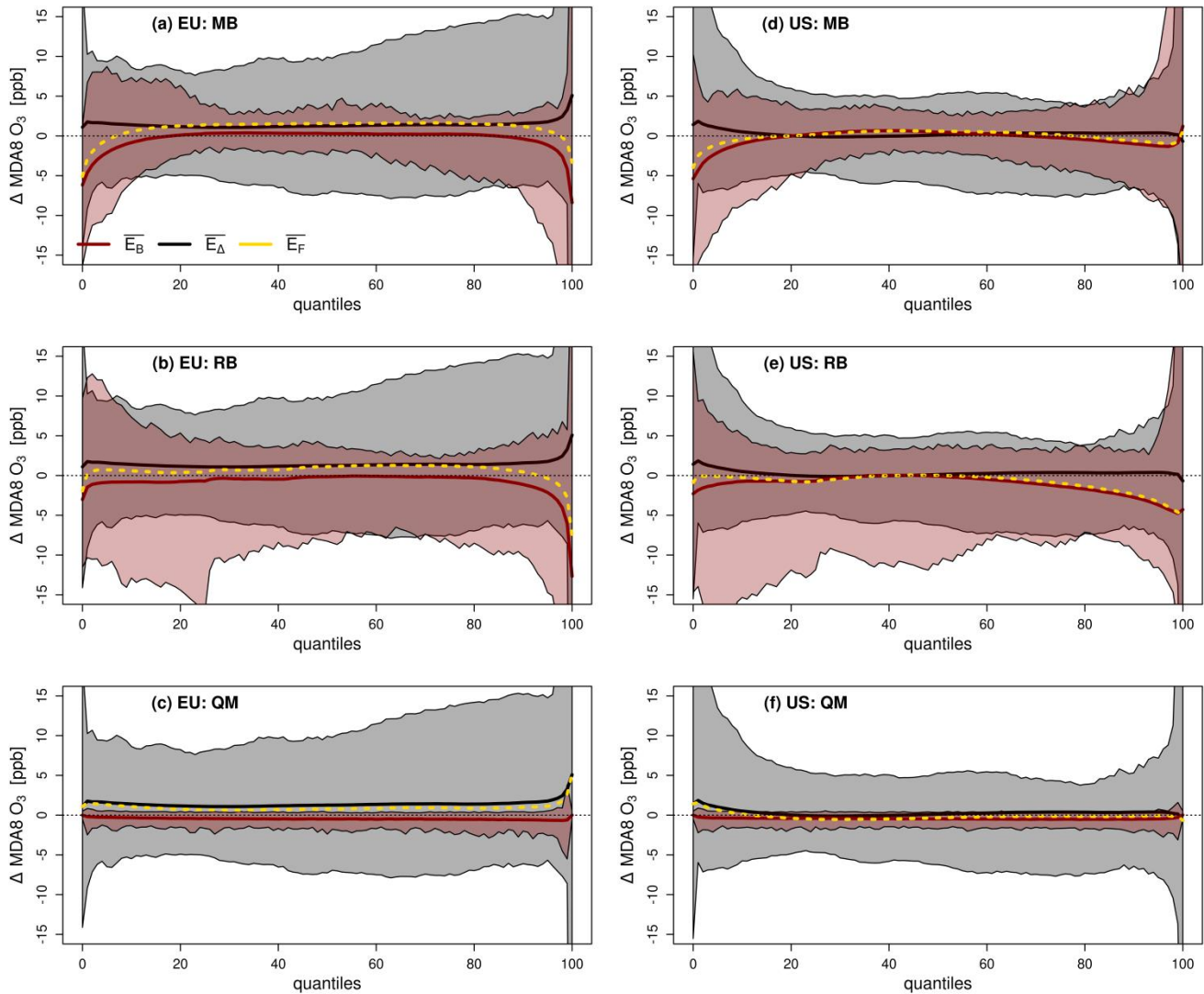
Fig. 5: Error Components of the CESM2-WACCM6 model during the evaluation period, for the MB (a & d), RB (b & e) and QM (c & f) methods, in the EU (left column) and US (right column) domain. The red shading gives the minimum to maximum range, and the solid red line the domain average of the residual bias in the base period (E_B), respectively. The grey shading gives the minimum to maximum range and the solid black line the domain average of the differences in the change between the base and evaluation period of the raw model and observations (E_Δ), respectively. The resulting domain average error of the evaluation period (E_F) is indicated by the dashed yellow line (note, for the DC method $E_B = 0$ and hence $E_F = E_\Delta$).

3.4 The influence of meteorology on the bias in the CESM2-WACCM6 ensemble

Having illustrated the MDA8 O_3 biases of various CMIP6 models, the performance of various statistical bias techniques as well as the influence of the model response to changes in e.g. emissions on the performance of bias correction we turn here to shed light on the underlying cause of biased MDA8 O_3 model outputs. To this end we ~~analyse~~analyze the 13 members of the CESM2-WACCM6 ensemble in more detail, in order to examine for consistency within the individual realizations as

well as a possible dominant cause(s) for the bias in the modelled surface ozone fields. Here two likely prime candidates exist: 1) issues with the sensitivity in chemical mechanisms to local/regional precursor emissions (note, anthropogenic emissions are consistent across individual models), 2) issues in meteorology simulated by~~ical driving in~~ the free running CCM. For the latter, we further include three~~wo~~ climatological key drivers for ozone production/accumulation in our analysis, i.e. daily maximum temperature (TSMX), ~~and~~ daily average down welling short wave radiation (FSDS) and daily average wind speed (WSPD), in order to differentiate whether the bias is predominantly driven by sensitivity to meteorology or chemistry. As chemical covariates we include monthly averages of NO, NO_2 and HCHO, the latter we consider as bulk proxy for VOCs ~~(e.g. Shen et al., 2019; Zhu et al., 2017)~~[e.g. Shen et al., 2019; Zhu et al., 2017].

Figures 6 and 7 illustrate~~s~~ the PDFs of MDA8 O_3, NO, NO_2, HCHO, TSMX, ~~and~~ FSDS, and WSPD for the individual ensemble members during spring and summer in 2005-2009 (the PDFs for 2010-2014 are shown in ~~the~~ supplemental Fig. S11 and S12). MAM and JJA MDA8 O_3 (Fig. 6a,d~~e~~) show a very similar distribution across ensemble members for both domains. For example the median MDA8 O_3 value ranges across ensemble members roughly between 50 and 52 ppb (MAM) and 45 to 47 ppb (JJA) in the EU. For the US the median MDA8 O_3 values are found to be slightly higher than in the EU, but the differences within the ensemble lie in the same narrow range (53 to 55 ppb for MAM and 54 to 55 ppb for JJA). Similarly, compact PDFs across the ensemble are found for NO, NO_2 and HCHO. Interestingly differences emerge for HCHO in the US but not Europe which represents a larger influence of biogenic emissions.

~~In context of the meteorological variables s~~Similar results are found for the meteorological variables. Although~~,~~ slight variations occur for surface temperature, ~~and~~ radiation, and wind speed (which one would expect from a model ~~with free running~~generating its own meteorology), the PDFs are widely homogenous across the ensemble, thereby explaining ~~as all ensemble members are driven with the same set of precursor emissions,~~ the similarity of surface ozone distributions within the ensemble (as all ensemble members are driven with the same set of precursor emissions) in both domains. The analysis of the MDA8 O_3, NO, NO_2, HCHO, TSMX, ~~and~~ FSDS, and WSPD distributions over the second time period (2010-2014, Fig~~s~~. S11 and S12) yields similar results, thereby providing confidence for the robustness of our findings.

The strong similarity across ensemble members indicates that the MDA8 O_3 bias identified in CESM2-WACCM6 stems most likely from sensitivities in the chemical mechanism and/or emissions and not from meteorological drivers and their variability. As the models use the same anthropogenic emissions, the differences are more likely to stem from the chemistry, which could include different mixes of emitted VOCs. Previous research has shown that temperature biases are rather small and that a significant overestimation of the temperature in the troposphere solely occurs in the southern hemisphere polar region, a region which is not investigated here [Danabasoglu et al., 2020; Gettelman et al., 2019]. Nevertheless, we note that small deviations in temperature have been found to explain biases of 5-15 ppb for surface O_3 in former model generations [Rasmussen et al., 2012]. While the presented ensemble analysis is, due to data availability, only possible for CESM2-WACCM6, the results provide a first order estimate of the dominant model component responsible for surface ozone biases. Future work should confirm that this finding holds for other global models and thus an ensemble strategy for model experiments is recommended for future model intercomparison activities such as CCMI and CMIP.
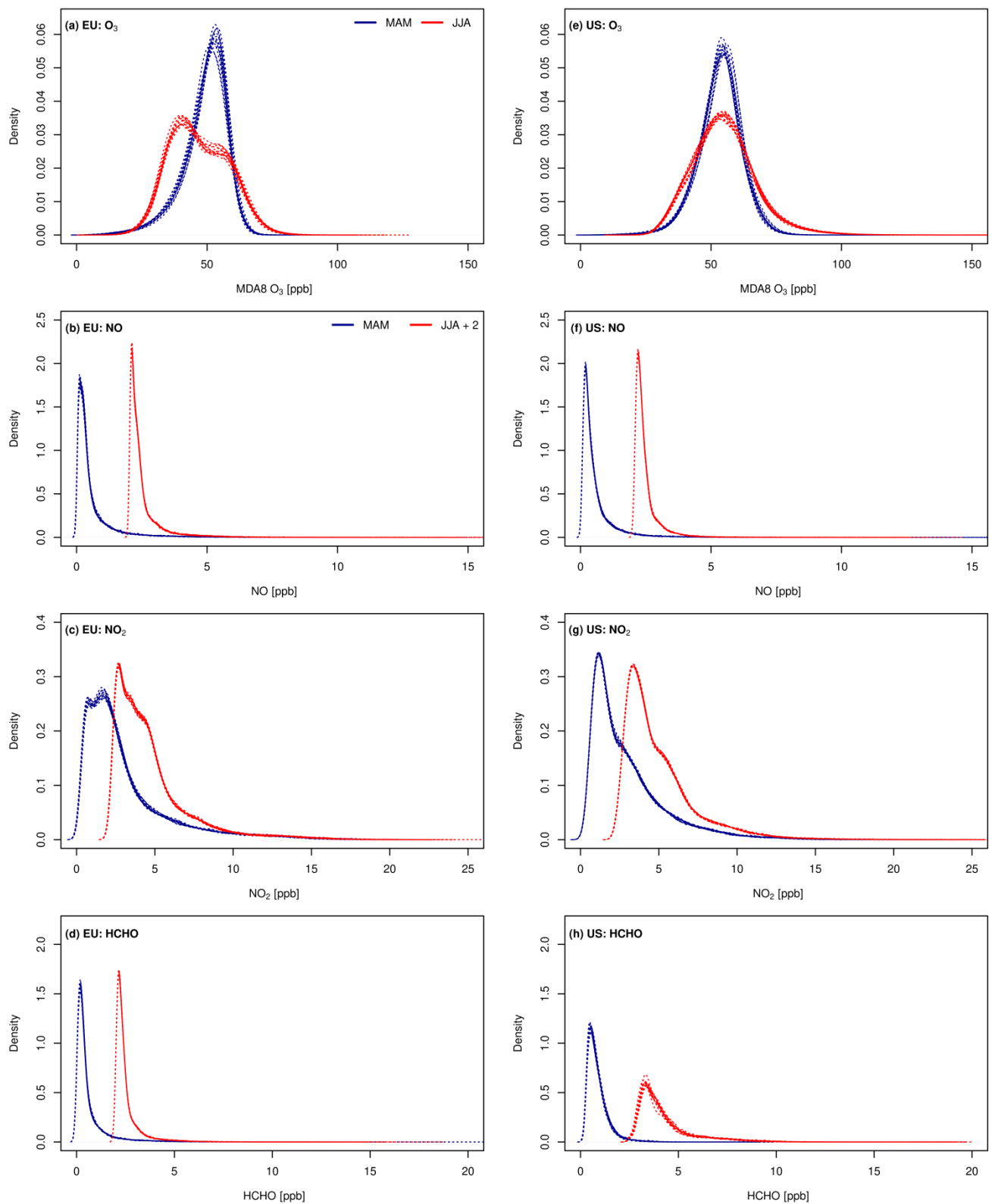
Fig. 6: CESM2-WACCM6 spring (MAM) and summer time (JJA) PDFs of (a) MDA8 O$_3$, (b) NO, (c) NO$_2$, (d) HCHO ~~TSMX and FSDS~~ for the European ~~(left) and US (right)~~ domain in 2005-2009. (e)-(h) as (a)-(b) but for the US domain Note, a ~~factor~~value of 2 has been added to summertime concentrations of NO, NO$_2$ and HCHO ~~have been multiplied with a factor of 2~~ to allow for visual separation of the seasonal PDFs.

385
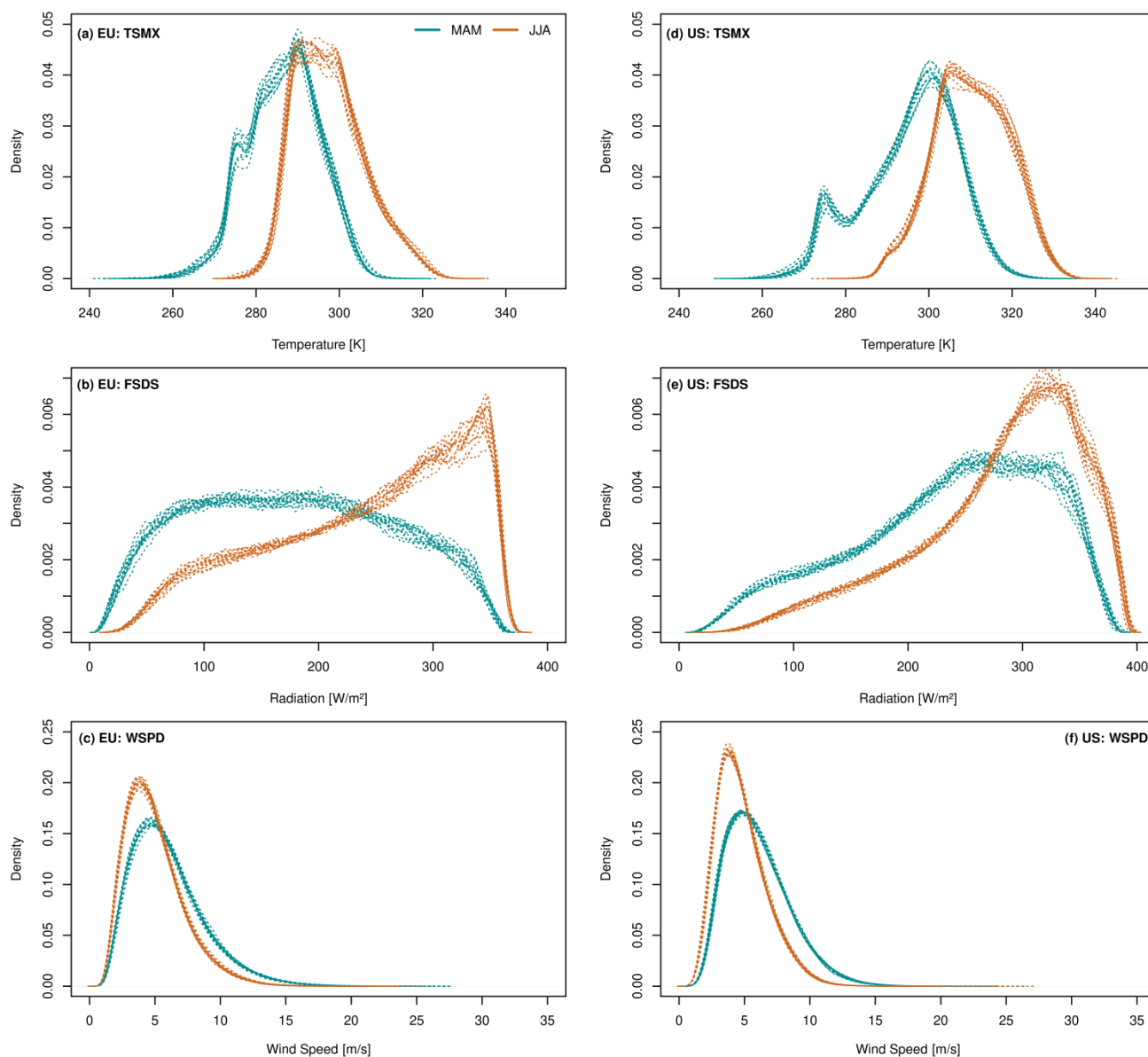
Fig. 7: CESM2-WACCM6 spring (MAM) and summer time (JJA) PDFs of (a) TSMX, (b) FSDS, and (c) WSPD for the European (left) and US (right) domain in 2005-2009. (d)-(f) as (a)-(c) but for the US domain.

4 Summary & Conclusions

In this study we evaluate four global CCMs contributing to CMIP6 (EC-Earth3, CESM2-WACCM6, GFDL-ESM4 and UKESM1-0-LL) regarding their bias in surface ozone burdens, and present the first comprehensive comparison of the performance of four different statistical bias correction techniques to derive CCM-based ozone metrics with relevance for public health and policy. While all models show biases when compared to observations, the bias magnitude of the raw, un-corrected MDA8 O_3 outputs differs strongly within the pool of models analyzed.

The evaluation of the four bias correction techniques for the base period (2005-2009), where techniques are tuned to observations, illustrates that all methods are capable to lower the bias. The MB and RB methods, however, are less accurate

when contrasted with the results obtained with the DC or QM approaches. Furthermore, when applying the MB and RB methods the model output fields might even be overcorrected for individual grid cells, i.e., the resulting ozone distributions might become biased low. This is not ~~astonishing,~~ surprising as both techniques apply a single average value for the correction of the whole distribution function, which is a disadvantage - especially when it comes to the tails of the distribution - if the bias is not constant across the ECDF.

The independent evaluation of the four techniques over the second time period (2010-2014), focusing on the bias correction of model projections, yields less distinct results. Although the model-­to-­observation agreement is improved for all MDA8 O_3 metrics in the corrected models compared to their raw counterparts, no single optimal correction technique can be identified. Our results illustrate that technique performance depends strongly on the model selected and its MDA8 O_3 evolution, and thus response to boundary condition~~s~~ changes, over time. This at first surprising result, however, can be explained by the examination of the composition of the residual model error.

The residual error for future projections is comprised of two parts: 1) the residual error of the base period E_B, and 2) the error attributable to the model response to changes in boundary conditions (emissions, climate, etc…) between both time periods E_Δ. ~~Especially t~~The magnitude of E_Δ was found to exert a dominant influence on the overall correction performance, which raises some concerns regarding the robustness of model responses and thus the reliability of model projections (not only in context of surface O_3). In contrast to E_Δ, E_B depends on the quality of the initial base period bias correction. Here our results clearly show that E_B is substantially larger for the MB and RB than the QM and DC methods. When applying the correction techniques E_Δ and E_B might compensate for individual grid cells, resulting in a low residual bias. On the contrary, the strong performance for the base period ~~performance~~ obtained with the QM and DC approaches are attributable to a very low E_B, which might deteriorate in projections if E_Δ is large. Thus, we conclude, that under the assumption of an adequate model response to changing boundary conditions (and thus low E_Δ), the QM and DC methods are outperforming the MB and RB techniques. If a decision has to be made whether the DC or QM approach is used for bias correction, we would argue, given that differences between the results obtained with both techniques are negligible, for DC correction due the comparably easy numerical implementation.

To obtain further insights of the root cause(s) of the bias surface ozone in models, we explored the MDA8 O_3 output of the 13 member CESM2-WACCM6 ensemble together with information on NO, NO_2 and HCHO as well as ~~the~~ key meteorological covariates for ozone production, i.e. daily maximum temperature, ~~and~~ daily mean incoming shortwave radiation and daily mean wind speed. Here our analysis showed only small variations within the CESM2-WACCM6 ensemble for core meteorological drivers (and chemical covariates) of surface ozone. This suggests, given that emissions are consistent across models, ~~rather~~ a dominant influence of the chemical mechanism ~~and/or considered emissions~~ on the bias in the O_3 fields rather than a prominent role for model meteorology. To investigate if this finding can be generalized to other CCMs ~~is planned for future work as it also~~ requires future community efforts ~~to in~~ in the provision of~~deding~~ additional ensemble simulations for individual CCMs contributing to the CCMI or CMIP frameworks.

Data availability

CMIP6 data sets are publicly available via https://esgf-data.dkrz.de/projects/cmip6-dkrz/. Processed data can be made available by the corresponding author upon reasonable request. The gridded MDA8 O_3 datasets are available at: https://doi.org/10.5281/zenodo.10832955

Author Contribution

C. Staehle: conceptualization, formal analysis, methodology, visualization, writing – original draft preparation

H. E. Rieder: conceptualization, methodology, resources, supervision, writing – review and editing

A. M. Fiore: resources, supervision, writing – review and editing

J. Schnell: data curation, writing – review and editing

Competing Interests

The authors declare that they have no conflict of interest.

Acknowledgement

The authors are grateful to the EC-Earth3, GFDL-ESM4 and UKESM1-0-LL modelling teams for providing the ensemble simulations via https://esgf-data.dkrz.de/projects/cmip6-dkrz/. and to J. Schnell for providing the gridded surface ozone data set. H.E. Rieder and C. Staehle acknowledge partial support by the Austrian Climate and Energy Fund via project ACRP11-KR18AC0K14686. C. Staehle acknowledges support through an OeAD Marietta Blau Fellowship grant. This research was supported in part by the NOAA cooperative agreement NA22OAR4320151, for the Cooperative Institute for Earth System Research and Data Science (CIESRDS). The statements, findings, conclusions, and recommendations are those of the author(s) and do not necessarily reflect the views of NOAA or the U.S. Department of Commerce. J.L. Schnell was supported in part by the NOAA cooperative agreement NA22OAR4320151. The authors are grateful to Ramiro Checa-Garcia for fruitful discussions and comments. The authors thank two anonymous reviewers for their valuable comments on an earlier version of this manuscript.

References

455   Akritidis, D., Zanis, P., Pytharoulis, I., Mavrakis, A., Karacostas, T. (2010). A deep stratospheric intrusion event down to the earth's surface of the megacity of Athens. *Meteorology and Atmospheric Physics, 109*(1), 9-18. doi:10.1007/s00703-010-0096-6

Archibald, A. T., Neu, J. L., Elshorbany, Y. F., Cooper, O. R., Young, P. J., Akiyoshi, H., Cox, R. A., Coyle, M., Derwent, R. G., Deushi, M., Finco, A., Frost, G. J., Galbally, I. E., Gerosa, G., Granier, C., Griffiths, P. T., Hossaini, R., Hu, L.,

460   Jöckel, P., Josse, B., Lin, M. Y., Mertens, M., Morgenstern, O., Naja, M., Naik, V., Oltmans, S., Plummer, D. A., Revell, L. E., Saiz-Lopez, A., Saxena, P., Shin, Y. M., Shahid, I., Shallcross, D., Tilmes, S., Trickl, T., Wallington, T. J., Wang, T., Worden, H. M., Zeng, G. (2020). Tropospheric Ozone Assessment Report: A critical review of changes in the tropospheric ozone burden and budget from 1850 to 2100. *Elementa: Science of the Anthropocene, 8*(1), 034. doi:10.1525/elementa.2020.034

465   Chameides, W. L., Lindsay, R. W., Richardson, J., Kiang, C. S. (1988). The Role of Biogenic Hydrocarbons in Urban Photochemical Smog: Atlanta as a Case Study. *Science, 241*(4872), 1473-1475. doi:10.1126/science.3420404

Checa-Garcia, R., Hegglin, M. I., Kinnison, D., Plummer, D. A., Shine, K. P. (2018). Historical Tropospheric and Stratospheric Ozone Radiative Forcing Using the CMIP6 Database. *Geophys Res Lett, 45*(7), 3264-3273. doi:10.1002/2017GL076770

470   Da, Y., Xu, Y., McCarl, B. (2022). Effects of Surface Ozone and Climate on Historical (1980–2015) Crop Yields in the United States: Implication for Mid-21st Century Projection. *Environmental and Resource Economics, 81*(2), 355-378. doi:10.1007/s10640-021-00629-y

Danabasoglu, G., Lamarque, J. F., Bacmeister, J., Bailey, D. A., DuVivier, A. K., Edwards, J., Emmons, L. K., Fasullo, J., Garcia, R., Gettelman, A., Hannay, C., Holland, M. M., Large, W. G., Lauritzen, P. H., Lawrence, D. M., Lenaerts,

475   J. T. M., Lindsay, K., Lipscomb, W. H., Mills, M. J., Neale, R., Oleson, K. W., Otto-Bliesner, B., Phillips, A. S., Sacks, W., Tilmes, S., van Kampenhout, L., Vertenstein, M., Bertini, A., Dennis, J., Deser, C., Fischer, C., Fox-Kemper, B., Kay, J. E., Kinnison, D., Kushner, P. J., Larson, V. E., Long, M. C., Mickelson, S., Moore, J. K., Nienhouse, E., Polvani, L., Rasch, P. J., Strand, W. G. (2020). The Community Earth System Model Version 2 (CESM2). *J Adv Model Earth Sy, 12*(2), e2019MS001916. doi:10.1029/2019MS001916

480   Ducker, J. A., Holmes, C. D., Keenan, T. F., Fares, S., Goldstein, A. H., Mammarella, I., Munger, J. W., Schnell, J. (2018). Synthetic ozone deposition and stomatal uptake at flux tower sites. *Biogeosciences, 15*(17), 5395-5413. doi:10.5194/bg-15-5395-2018

EEA. (2020). *Air quality in Europe - 2020 Report* (09/2020). Retrieved from https://www.eea.europa.eu/publications/air-quality-in-europe-2020-report

485   EPA. (2015). *National Ambient Air Quality Standards for Ozone*. Retrieved from https://www.govinfo.gov/content/pkg/FR-2015-10-26/pdf/2015-26594.pdf

EUR-LEX. (2008). *Directive 2008/50/EC of the European parliament and of the council of 21 May 2008 on ambient air quality and cleaner air for Europe* (2008/50/EC). Retrieved from https://eur-lex.europa.eu/legal-content/EN/TXT/?uri=CELEX:32008L0050

490   EUR-LEX. (2011). *Commission Implementing Decision of 12 December 2011 laying down rules for Directives 2004/107/EC and 2008/50/EC of the European Parliament and of the Council as regards the reciprocal exchange*

of information and reporting on ambient air quality (notified under document C(2011) 9068) (2011/850/EU). Retrieved from http://data.europa.eu/eli/dec_impl/2011/850/2011-12-17

Fleming, Z. L., Doherty, R. M., von Schneidemesser, E., Malley, C. S., Cooper, O. R., Pinto, J. P., Colette, A., Xu, X., Simpson, D., Schultz, M. G., Lefohn, A. S., Hamad, S., Moolla, R., Solberg, S., Feng, Z. (2018). Tropospheric Ozone Assessment Report: Present-day ozone distribution and trends relevant to human health. *Elementa: Science of the Anthropocene, 6*, 12. doi:10.1525/elementa.273

Garrido-Perez, J. M., Ordóñez, C., García-Herrera, R., Schnell, J. L. (2019). The differing impact of air stagnation on summer ozone across Europe. *Atmospheric Environment, 219*, 117062. doi:10.1016/j.atmosenv.2019.117062

Gettelman, A., Mills, M. J., Kinnison, D. E., Garcia, R. R., Smith, A. K., Marsh, D. R., Tilmes, S., Vitt, F., Bardeen, C. G., McInerny, J., Liu, H. L., Solomon, S. C., Polvani, L. M., Emmons, L. K., Lamarque, J. F., Richter, J. H., Glanville, A. S., Bacmeister, J. T., Phillips, A. S., Neale, R. B., Simpson, I. R., DuVivier, A. K., Hodzic, A., Randel, W. J. (2019). The Whole Atmosphere Community Climate Model Version 6 (WACCM6). *J Geophys Res-Atmos, 124*(23), 12380-12403. doi:10.1029/2019JD030943

Griffiths, P. T., Murray, L. T., Zeng, G., Shin, Y. M., Abraham, N. L., Archibald, A. T., Deushi, M., Emmons, L. K., Galbally, I. E., Hassler, B., Horowitz, L. W., Keeble, J., Liu, J., Moeini, O., Naik, V., O'Connor, F. M., Oshima, N., Tarasick, D., Tilmes, S., Turnock, S. T., Wild, O., Young, P. J., Zanis, P. (2021). Tropospheric ozone in CMIP6 simulations. *Atmos Chem Phys, 21*(5), 4187-4218. doi:10.5194/acp-21-4187-2021

Gu, Y., Henze, D. K., Nawaz, M. O., Wagner, U. J. (2023). Response of the ozone-related health burden in Europe to changes in local anthropogenic emissions of ozone precursors. *Environmental Research Letters, 18*(11), 114034. doi:10.1088/1748-9326/ad0167

Guo, J. J., Fiore, A. M., Murray, L. T., Jaffe, D. A., Schnell, J. L., Moore, C. T., Milly, G. P. (2018). Average versus high surface ozone levels over the continental USA: model bias, background influences, and interannual variability. *Atmos. Chem. Phys., 18*(16), 12123-12140. doi:10.5194/acp-18-12123-2018

Karlický, J., Rieder, H. E., Huszár, P., Peiker, J., Sukhodolov, T. (2024). A cautious note advocating the use of ensembles of models and driving data in modeling of regional ozone burdens. *Air Quality, Atmosphere & Health*. doi:10.1007/s11869-024-01516-3

Lehner, F., Nadeem, I., Formayer, H. (2023). Evaluating skills and issues of quantile-based bias adjustment for climate change scenarios. *Adv Stat Clim Meteorol Oceanogr, 9*(1), 29-44. doi:10.5194/ascmo-9-29-2023

Lelieveld, J., Dentener, F. J. (2000). What controls tropospheric ozone? *J Geophys Res-Atmos, 105*(D3), 3531-3551. doi:10.1029/1999JD901011

Lin, M., Fiore, A. M., Horowitz, L. W., Langford, A. O., Oltmans, S. J., Tarasick, D., Rieder, H. E. (2015). Climate variability modulates western US ozone air quality in spring via deep stratospheric intrusions. *Nature Communications, 6*(1), 7105. doi:10.1038/ncomms8105

Liu, Z., Doherty, R. M., Wild, O., O'Connor, F. M., Turnock, S. T. (2022). Correcting ozone biases in a global chemistry–climate model: implications for future ozone. *Atmos Chem Phys, 22*(18), 12543-12557. doi:10.5194/acp-22-12543-2022

Malashock, D. A., Delang, M. N., Becker, J. S., Serre, M. L., West, J. J., Chang, K.-L., Cooper, O. R., Anenberg, S. C. (2022). Global trends in ozone concentration and attributable mortality for urban, peri-urban, and rural areas

530   between 2000 and 2019: a modelling study. *The Lancet Planetary Health, 6*(12), e958-e967. doi:10.1016/S2542-5196(22)00260-1

Meehl, G. A., Tebaldi, C., Tilmes, S., Lamarque, J.-F., Bates, S., Pendergrass, A., Lombardozzi, D. (2018). Future heat waves and surface ozone. *Environ Res Lett, 13*(6), 064004. doi:10.1088/1748-9326/aabcdc

Mills, G., Pleijel, H., Malley, C. S., Sinha, B., Cooper, O. R., Schultz, M. G., Neufeld, H. S., Simpson, D., Sharps, K., Feng,
535   Z., Gerosa, G., Harmens, H., Kobayashi, K., Saxena, P., Paoletti, E., Sinha, V., Xu, X. (2018). Tropospheric Ozone Assessment Report: Present-day tropospheric ozone distribution and trends relevant to vegetation. *Elementa: Science of the Anthropocene, 6*, 47. doi:10.1525/elementa.302

Monks, P. S., Archibald, A. T., Colette, A., Cooper, O., Coyle, M., Derwent, R., Fowler, D., Granier, C., Law, K. S., Mills, G. E., Stevenson, D. S., Tarasova, O., Thouret, V., von Schneidemesser, E., Sommariva, R., Wild, O., Williams, M.
540   L. (2015). Tropospheric ozone and its precursors from the urban to the global scale from air quality to short-lived climate forcer. *Atmos Chem Phys, 15*(15), 8889-8973. doi:10.5194/acp-15-8889-2015

Murray, C. J. L., Aravkin, A. Y., Zheng, P., Abbafati, C., Abbas, K. M., Abbasi-Kangevari, M., Abd-Allah, F., Abdelalim, A., Abdollahi, M., Abdollahpour, I., Abegaz, K. H., Abolhassani, H., Aboyans, V., Abreu, L. G., Abrigo, M. R. M., Abualhasan, A., Abu-Raddad, L. J., Abushouk, A. I., Adabi, M., Adekanmbi, V., Adeoye, A. M., Adetokunboh, O.
545   O., Adham, D., Advani, S. M., Agarwal, G., Aghamir, S. M. K., Agrawal, A., Ahmad, T., Ahmadi, K., Ahmadi, M., Ahmadieh, H., Ahmed, M. B., Akalu, T. Y., Akinyemi, R. O., Akinyemiju, T., Akombi, B., Akunna, C. J., Alahdab, F., Al-Aly, Z., Alam, K., Alam, S., Alam, T., Alanezi, F. M., Alanzi, T. M., Alemu, B. w., Alhabib, K. F., Ali, M., Ali, S., Alicandro, G., Alinia, C., Alipour, V., Alizade, H., Aljunid, S. M., Alla, F., Allebeck, P., Almasi-Hashiani, A., Al-Mekhlafi, H. M., Alonso, J., Altirkawi, K. A., Amini-Rarani, M., Amiri, F., Amugsi, D. A., Ancuceanu, R.,
550   Anderlini, D., Anderson, J. A., Andrei, C. L., Andrei, T., Angus, C., Anjomshoa, M., Ansari, F., Ansari-Moghaddam, A., Antonazzo, I. C., Antonio, C. A. T., Antony, C. M., Antriyandarti, E., Anvari, D., Anwer, R., Appiah, S. C. Y., Arabloo, J., Arab-Zozani, M., Ariani, F., Armoon, B., Ärnlöv, J., Arzani, A., Asadi-Aliabadi, M., Asadi-Pooya, A. A., Ashbaugh, C., Assmus, M., Atafar, Z., Atnafu, D. D., Atout, M. M. d. W., Ausloos, F., Ausloos, M., Ayala Quintanilla, B. P., Ayano, G., Ayanore, M. A., Azari, S., Azarian, G., Azene, Z. N., Badawi, A., Badiye,
555   A. D., Bahrami, M. A., Bakhshaei, M. H., Bakhtiari, A., Bakkannavar, S. M., Baldasseroni, A., Ball, K., Ballew, S. H., Balzi, D., Banach, M., Banerjee, S. K., Bante, A. B., Baraki, A. G., Barker-Collo, S. L., Bärnighausen, T. W., Barrero, L. H., Barthelemy, C. M., Barua, L., Basu, S., Baune, B. T., Bayati, M., Becker, J. S., Bedi, N., Beghi, E., Béjot, Y., Bell, M. L., Bennitt, F. B., Bensenor, I. M., Berhe, K., Berman, A. E., Bhagavathula, A. S., Bhageerathy, R., Bhala, N., Bhandari, D., Bhattacharyya, K., Bhutta, Z. A., Bijani, A., Bikbov, B., Bin Sayeed, M. S., Biondi, A.,
560   Birihane, B. M., Bisignano, C., Biswas, R. K., Bitew, H., Bohlouli, S., Bohluli, M., Boon-Dooley, A. S., Borges, G., Borzì, A. M., Borzouei, S., Bosetti, C., Boufous, S., Braithwaite, D., Breitborde, N. J. K., Breitner, S., Brenner, H., Briant, P. S., Briko, A. N., Briko, N. I., Britton, G. B., Bryazka, D., Bumgarner, B. R., Burkart, K., Burnett, R. T., Burugina Nagaraja, S., Butt, Z. A., Caetano dos Santos, F. L., Cahill, L. E., Cámera, L. L. A. A., Campos-Nonato, I. R., Cárdenas, R., Carreras, G., Carrero, J. J., Carvalho, F., Castaldelli-Maia, J. M., Castañeda-Orjuela, C.
565   A., Castelpietra, G., Castro, F., Causey, K., Cederroth, C. R., Cercy, K. M., Cerin, E., Chandan, J. S., Chang, K.-L., Charlson, F. J., Chattu, V. K., Chaturvedi, S., Cherbuin, N., Chimed-Ochir, O., Cho, D. Y., Choi, J.-Y. J., Christensen, H., Chu, D.-T., Chung, M. T., Chung, S.-C., Cicuttini, F. M., Ciobanu, L. G., Cirillo, M., Classen, T. K. D., Cohen, A. J., Compton, K., Cooper, O. R., Costa, V. M., Cousin, E., Cowden, R. G., Cross, D. H., Cruz, J.

570 A., Dahlawi, S. M. A., Damasceno, A. A. M., Damiani, G., Dandona, L., Dandona, R., Dangel, W. J., Danielsson, A.-K., Dargan, P. I., Darwesh, A. M., Daryani, A., Das, J. K., Das Gupta, R., das Neves, J., Dávila-Cervantes, C. A., Davitoiu, D. V., De Leo, D., Degenhardt, L., DeLang, M., Dellavalle, R. P., Demeke, F. M., Demoz, G. T., Demsie, D. G., Denova-Gutiérrez, E., Dervenis, N., Dhungana, G. P., Dianatinasab, M., Dias da Silva, D., Diaz, D., Dibaji Forooshani, Z. S., Djalalinia, S., Do, H. T., Dokova, K., Dorostkar, F., Doshmangir, L., Driscoll, T. R., Duncan, B. B., Duraes, A. R., Eagan, A. W., Edvardsson, D., El Nahas, N., El Sayed, I., El Tantawi, M., Elbarazi,

575 I., Elgendy, I. Y., El-Jaafary, S. I., Elyazar, I. R. F., Emmons-Bell, S., Erskine, H. E., Eskandarieh, S., Esmaeilnejad, S., Esteghamati, A., Estep, K., Etemadi, A., Etisso, A. E., Fanzo, J., Farahmand, M., Fareed, M., Faridnia, R., Farioli, A., Faro, A., Faruque, M., Farzadfar, F., Fattahi, N., Fazlzadeh, M., Feigin, V. L., Feldman, R., Fereshtehnejad, S.-M., Fernandes, E., Ferrara, G., Ferrari, A. J., Ferreira, M. L., Filip, I., Fischer, F., Fisher, J. L., Flor, L. S., Foigt, N. A., Folayan, M. O., Fomenkov, A. A., Force, L. M., Foroutan, M., Franklin, R. C., Freitas, M.,

580 Fu, W., Fukumoto, T., Furtado, J. M., Gad, M. M., Gakidou, E., Gallus, S., Garcia-Basteiro, A. L., Gardner, W. M., Geberemariyam, B. S., Gebreslassie, A. A. A. A., Geremew, A., Gershberg Hayoon, A., Gething, P. W., Ghadimi, M., Ghadiri, K., Ghaffarifar, F., Ghafourifard, M., Ghamari, F., Ghashghaee, A., Ghiasvand, H., Ghith, N., Gholamian, A., Ghosh, R., Gill, P. S., Ginindza, T. G. G., Giussani, G., Gnedovskaya, E. V., Goharinezhad, S., Gopalani, S. V., Gorini, G., Goudarzi, H., Goulart, A. C., Greaves, F., Grivna, M., Grosso, G., Gubari, M. I. M.,

585 Gugnani, H. C., Guimarães, R. A., Guled, R. A., Guo, G., Guo, Y., Gupta, R., Gupta, T., Haddock, B., Hafezi-Nejad, N., Hafiz, A., Haj-Mirzaian, A., Haj-Mirzaian, A., Hall, B. J., Halvaei, I., Hamadeh, R. R., Hamidi, S., Hammer, M. S., Hankey, G. J., Haririan, H., Haro, J. M., Hasaballah, A. I., Hasan, M. M., Hasanpoor, E., Hashi, A., Hassanipour, S., Hassankhani, H., Havmoeller, R. J., Hay, S. I., Hayat, K., Heidari, G., Heidari-Soureshjani, R., Henrikson, H. J., Herbert, M. E., Herteliu, C., Heydarpour, F., Hird, T. R., Hoek, H. W., Holla, R., Hoogar, P.,

590 Hosgood, H. D., Hossain, N., Hosseini, M., Hosseinzadeh, M., Hostiuc, M., Hostiuc, S., Househ, M., Hsairi, M., Hsieh, V. C.-r., Hu, G., Hu, K., Huda, T. M., Humayun, A., Huynh, C. K., Hwang, B.-F., Iannucci, V. C., Ibitoye, S. E., Ikeda, N., Ikuta, K. S., Ilesanmi, O. S., Ilic, I. M., Ilic, M. D., Inbaraj, L. R., Ippolito, H., Iqbal, U., Irvani, S. S. N., Irvine, C. M. S., Islam, M. M., Islam, S. M. S., Iso, H., Ivers, R. Q., Iwu, C. C. D., Iwu, C. J., Iyamu, I. O., Jaafari, J., Jacobsen, K. H., Jafari, H., Jafarinia, M., Jahani, M. A., Jakovljevic, M., Jalilian, F., James, S. L.,

595 Janjani, H., Javaheri, T., Javidnia, J., Jeemon, P., Jenabi, E., Jha, R. P., Jha, V., Ji, J. S., Johansson, L., John, O., John-Akinola, Y. O., Johnson, C. O., Jonas, J. B., Joukar, F., Jozwiak, J. J., Jürisson, M., Kabir, A., Kabir, Z., Kalani, H., Kalani, R., Kalankesh, L. R., Kalhor, R., Kanchan, T., Kapoor, N., Karami Matin, B., Karch, A., Karim, M. A., Kassa, G. M., Katikireddi, S. V., Kayode, G. A., Kazemi Karyani, A., Keiyoro, P. N., Keller, C., Kemmer, L., Kendrick, P. J., Khalid, N., Khammarnia, M., Khan, E. A., Khan, M., Khatab, K., Khater, M. M., Khatib, M. N.,

600 Khayamzadeh, M., Khazaei, S., Kieling, C., Kim, Y. J., Kimokoti, R. W., Kisa, A., Kisa, S., Kivimäki, M., Knibbs, L. D., Knudsen, A. K. S., Kocarnik, J. M., Kochhar, S., Kopec, J. A., Korshunov, V. A., Koul, P. A., Koyanagi, A., Kraemer, M. U. G., Krishan, K., Krohn, K. J., Kromhout, H., Kuate Defo, B., Kumar, G. A., Kumar, V., Kurmi, O. P., Kusuma, D., La Vecchia, C., Lacey, B., Lal, D. K., Lalloo, R., Lallukka, T., Lami, F. H., Landires, I., Lang, J. J., Langan, S. M., Larsson, A. O., Lasrado, S., Lauriola, P., Lazarus, J. V., Lee, P. H., Lee, S. W. H., LeGrand, K. E.,

605 Leigh, J., Leonardi, M., Lescinsky, H., Leung, J., Levi, M., Li, S., Lim, L.-L., Linn, S., Liu, S., Liu, S., Liu, Y., Lo, J., Lopez, A. D., Lopez, J. C. F., Lopukhov, P. D., Lorkowski, S., Lotufo, P. A., Lu, A., Lugo, A., Maddison, E. R., Mahasha, P. W., Mahdavi, M. M., Mahmoudi, M., Majeed, A., Maleki, A., Maleki, S., Malekzadeh, R., Malta, D.

C., Mamun, A. A., Manda, A. L., Manguerra, H., Mansour-Ghanaei, F., Mansouri, B., Mansournia, M. A., Mantilla Herrera, A. M., Maravilla, J. C., Marks, A., Martin, R. V., Martini, S., Martins-Melo, F. R., Masaka, A., Masoumi, S. Z., Mathur, M. R., Matsushita, K., Maulik, P. K., McAlinden, C., McGrath, J. J., McKee, M., Mehndiratta, M. M., Mehri, F., Mehta, K. M., Memish, Z. A., Mendoza, W., Menezes, R. G., Mengesha, E. W., Mereke, A., Mereta, S. T., Meretoja, A., Meretoja, T. J., Mestrovic, T., Miazgowski, B., Miazgowski, T., Michalek, I. M., Miller, T. R., Mills, E. J., Mini, G. K., Miri, M., Mirica, A., Mirrakhimov, E. M., Mirzaei, H., Mirzaei, M., Mirzaei, R., Mirzaei-Alavijeh, M., Misganaw, A. T., Mithra, P., Moazen, B., Mohammad, D. K., Mohammad, Y., Mohammad Gholi Mezerji, N., Mohammadian-Hafshejani, A., Mohammadifard, N., Mohammadpourhodki, R., Mohammed, A. S., Mohammed, H., Mohammed, J. A., Mohammed, S., Mokdad, A. H., Molokhia, M., Monasta, L., Mooney, M. D., Moradi, G., Moradi, M., Moradi-Lakeh, M., Moradzadeh, R., Moraga, P., Morawska, L., Morgado-da-Costa, J., Morrison, S. D., Mosapour, A., Mosser, J. F., Mouodi, S., Mousavi, S. M., Mousavi Khaneghah, A., Mueller, U. O., Mukhopadhyay, S., Mullany, E. C., Musa, K. I., Muthupandian, S., Nabhan, A. F., Naderi, M., Nagarajan, A. J., Nagel, G., Naghavi, M., Naghshtabrizi, B., Naimzada, M. D., Najafi, F., Nangia, V., Nansseu, J. R., Naserbakht, M., Nayak, V. C., Negoi, I., Ngunjiri, J. W., Nguyen, C. T., Nguyen, H. L. T., Nguyen, M., Nigatu, Y. T., Nikbakhsh, R., Nixon, M. R., Nnaji, C. A., Nomura, S., Norrving, B., Noubiap, J. J., Nowak, C., Nunez-Samudio, V., Oţoiu, A., Oancea, B., Odell, C. M., Ogbo, F. A., Oh, I.-H., Okunga, E. W., Oladnabi, M., Olagunju, A. T., Olusanya, B. O., Olusanya, J. O., Omer, M. O., Ong, K. L., Onwujekwe, O. E., Orpana, H. M., Ortiz, A., Osarenotor, O., Osei, F. B., Ostroff, S. M., Otstavnov, N., Otstavnov, S. S., Øverland, S., Owolabi, M. O., P A, M., Padubidri, J. R., Palladino, R., Panda-Jonas, S., Pandey, A., Parry, C. D. H., Pasovic, M., Pasupula, D. K., Patel, S. K., Pathak, M., Patten, S. B., Patton, G. C., Pazoki Toroudi, H., Peden, A. E., Pennini, A., Pepito, V. C. F., Peprah, E. K., Pereira, D. M., Pesudovs, K., Pham, H. Q., Phillips, M. R., Piccinelli, C., Pilz, T. M., Piradov, M. A., Pirsaheb, M., Plass, D., Polinder, S., Polkinghorne, K. R., Pond, C. D., Postma, M. J., Pourjafar, H., Pourmalek, F., Poznańska, A., Prada, S. I., Prakash, V., Pribadi, D. R. A., Pupillo, E., Quazi Syed, Z., Rabiee, M., Rabiee, N., Radfar, A., Rafiee, A., Raggi, A., Rahman, M. A., Rajabpour-Sanati, A., Rajati, F., Rakovac, I., Ram, P., Ramezanzadeh, K., Ranabhat, C. L., Rao, P. C., Rao, S. J., Rashedi, V., Rathi, P., Rawaf, D. L., Rawaf, S., Rawal, L., Rawassizadeh, R., Rawat, R., Razo, C., Redford, S. B., Reiner, R. C., Jr., Reitsma, M. B., Remuzzi, G., Renjith, V., Renzaho, A. M. N., Resnikoff, S., Rezaei, N., Rezaei, N., Rezapour, A., Rhinehart, P.-A., Riahi, S. M., Ribeiro, D. C., Ribeiro, D., Rickard, J., Rivera, J. A., Roberts, N. L. S., Rodríguez-Ramírez, S., Roever, L., Ronfani, L., Room, R., Roshandel, G., Roth, G. A., Rothenbacher, D., Rubagotti, E., Rwegerera, G. M., Sabour, S., Sachdev, P. S., Saddik, B., Sadeghi, E., Sadeghi, M., Saeedi, R., Saeedi Moghaddam, S., Safari, Y., Safi, S., Safiri, S., Sagar, R., Sahebkar, A., Sajadi, S. M., Salam, N., Salamati, P., Salem, H., Salem, M. R. R., Salimzadeh, H., Salman, O. M., Salomon, J. A., Samad, Z., Samadi Kafil, H., Sambala, E. Z., Samy, A. M., Sanabria, J., Sánchez-Pimienta, T. G., Santomauro, D. F., Santos, I. S., Santos, J. V., Santric-Milicevic, M. M., Saraswathy, S. Y. I., Sarmiento-Suárez, R., Sarrafzadegan, N., Sartorius, B., Sarveazad, A., Sathian, B., Sathish, T., Sattin, D., Saxena, S., Schaeffer, L. E., Schiavolin, S., Schlaich, M. P., Schmidt, M. I., Schutte, A. E., Schwebel, D. C., Schwendicke, F., Senbeta, A. M., Senthilkumaran, S., Sepanlou, S. G., Serdar, B., Serre, M. L., Shadid, J., Shafaat, O., Shahabi, S., Shaheen, A. A., Shaikh, M. A., Shalash, A. S., Shams-Beyranvand, M., Shamsizadeh, M., Sharafi, K., Sheikh, A., Sheikhtaheri, A., Shibuya, K., Shield, K. D., Shigematsu, M., Shin, J. I., Shin, M.-J., Shiri, R., Shirkoohi, R., Shuval, K., Siabani, S., Sierpinski, R., Sigfusdottir, I. D., Sigurvinsdottir, R., Silva, J. P., Simpson, K. E., Singh, J. A., Singh, P., Skiadaresi,

E., Skou, S. T., Skryabin, V. Y., Smith, E. U. R., Soheili, A., Soltani, S., Soofi, M., Sorensen, R. J. D., Soriano, J. B., Sorrie, M. B., Soshnikov, S., Soyiri, I. N., Spencer, C. N., Spotin, A., Sreeramareddy, C. T., Srinivasan, V., Stanaway, J. D., Stein, C., Stein, D. J., Steiner, C., Stockfelt, L., Stokes, M. A., Straif, K., Stubbs, J. L., Sufiyan, M. a. B., Suleria, H. A. R., Suliankatchi Abdulkader, R., Sulo, G., Sultan, I., Szumowski, Ł., Tabarés-Seisdedos, R., Tabb, K. M., Tabuchi, T., Taherkhani, A., Tajdini, M., Takahashi, K., Takala, J. S., Tamiru, A. T., Taveira, N., Tehrani-Banihashemi, A., Temsah, M.-H., Tesema, G. A., Tessema, Z. T., Thurston, G. D., Titova, M. V., Tohidinik, H. R., Tonelli, M., Topor-Madry, R., Topouzis, F., Torre, A. E., Touvier, M., Tovani-Palone, M. R. R., Tran, B. X., Travillian, R., Tsatsakis, A., Tudor Car, L., Tyrovolas, S., Uddin, R., Umeokonkwo, C. D., Unnikrishnan, B., Upadhyay, E., Vacante, M., Valdez, P. R., van Donkelaar, A., Vasankari, T. J., Vasseghian, Y., Veisani, Y., Venketasubramanian, N., Violante, F. S., Vlassov, V., Vollset, S. E., Vos, T., Vukovic, R., Waheed, Y., Wallin, M. T., Wang, Y., Wang, Y.-P., Watson, A., Wei, J., Wei, M. Y. W., Weintraub, R. G., Weiss, J., Werdecker, A., West, J. J., Westerman, R., Whisnant, J. L., Whiteford, H. A., Wiens, K. E., Wolfe, C. D. A., Wozniak, S. S., Wu, A.-M., Wu, J., Wulf Hanson, S., Xu, G., Xu, R., Yadgir, S., Yahyazadeh Jabbari, S. H., Yamagishi, K., Yaminfirooz, M., Yano, Y., Yaya, S., Yazdi-Feyzabadi, V., Yeheyis, T. Y., Yilgwan, C. S., Yilma, M. T., Yip, P., Yonemoto, N., Younis, M. Z., Younker, T. P., Yousefi, B., Yousefi, Z., Yousefinezhadi, T., Yousuf, A. Y., Yu, C., Yusefzadeh, H., Zahirian Moghadam, T., Zamani, M., Zamanian, M., Zandian, H., Zastrozhin, M. S., Zhang, Y., Zhang, Z.-J., Zhao, J. T., Zhao, X.-J. G., Zhao, Y., Zhou, M., Ziapour, A., Zimsen, S. R. M., Brauer, M., Afshin, A., Lim, S. S. (2020). Global burden of 87 risk factors in 204 countries and territories, 1990-2019: a systematic analysis for the Global Burden of Disease Study 2019. *The Lancet, 396*(10258), 1223-1249. doi:10.1016/S0140-6736(20)30752-2

Nolte, C. G., Spero, T. L., Bowden, J. H., Mallard, M. S., Dolwick, P. D. (2018). The potential effects of climate change on air quality across the conterminous US at 2030 under three Representative Concentration Pathways. *Atmos. Chem. Phys., 18*(20), 15471-15489. doi:10.5194/acp-18-15471-2018

Pozzer, A., Anenberg, S. C., Dey, S., Haines, A., Lelieveld, J., Chowdhury, S. (2023). Mortality Attributable to Ambient Air Pollution: A Review of Global Estimates. *GeoHealth, 7*(1), e2022GH000711. doi:10.1029/2022GH000711

Rasmussen, D. J., Fiore, A. M., Naik, V., Horowitz, L. W., McGinnis, S. J., Schultz, M. G. (2012). Surface ozone-temperature relationships in the eastern US: A monthly climatology for evaluating chemistry-climate models. *Atmospheric Environment, 47*, 142-153. doi:10.1016/j.atmosenv.2011.11.021

Rieder, H. E., Fiore, A. M., Clifton, O. E., Correa, G., Horowitz, L. W., Naik, V. (2018). Combining model projections with site-level observations to estimate changes in distributions and seasonality of ozone in surface air over the U.S.A. *Atmos Environ, 193*, 302-315. doi:10.1016/j.atmosenv.2018.07.042

Rieder, H. E., Fiore, A. M., Horowitz, L. W., Naik, V. (2015). Projecting policy-relevant metrics for high summertime ozone pollution events over the eastern United States due to climate and emission changes during the 21st century. *J Geophys Res-Atmos, 120*(2), 784-800. doi:10.1002/2014JD022303

Schnell, J. L., Holmes, C. D., Jangam, A., Prather, M. J. (2014). Skill in forecasting extreme ozone pollution episodes with a global atmospheric chemistry model. *Atmos Chem Phys, 14*(15), 7721-7739. doi:10.5194/acp-14-7721-2014

Schnell, J. L., Prather, M. J. (2017). Co-occurrence of extremes in surface ozone, particulate matter, and temperature over eastern North America. *Proceedings of the National Academy of Sciences, 114*(11), 2854-2859. doi:10.1073/pnas.1614453114

Schnell, J. L., Prather, M. J., Josse, B., Naik, V., Horowitz, L. W., Cameron-Smith, P., Bergmann, D., Zeng, G., Plummer, D. A., Sudo, K., Nagashima, T., Shindell, D. T., Faluvegi, G., Strode, S. A. (2015). Use of North American and European air quality networks to evaluate global chemistry–climate modeling of surface ozone. *Atmos. Chem. Phys., 15*(18), 10581-10596. doi:10.5194/acp-15-10581-2015

Shen, L., Jacob, D. J., Zhu, L., Zhang, Q., Zheng, B., Sulprizio, M. P., Li, K., De Smedt, I., González Abad, G., Cao, H., Fu, T.-M., Liao, H. (2019). The 2005–2016 Trends of Formaldehyde Columns Over China Observed by Satellites: Increasing Anthropogenic Emissions of Volatile Organic Compounds and Decreasing Agricultural Fire Emissions. *Geophysical Research Letters, 46*(8), 4468-4475. doi:10.1029/2019GL082172

Sillman, S. (1999). The relation between ozone, NOx and hydrocarbons in urban and polluted rural environments. *Atmos Environ, 33*(12), 1821-1845. doi:10.1016/S1352-2310(98)00345-8

Sillman, S., Logan, J. A., Wofsy, S. C. (1990). The sensitivity of ozone to nitrogen oxides and hydrocarbons in regional ozone episodes. *J Geophy Res-Atmos, 95*(D2), 1837-1851. doi:10.1029/JD095iD02p01837

Stohl, A., Bonasoni, P., Cristofanelli, P., Collins, W., Feichter, J., Frank, A., Forster, C., Gerasopoulos, E., Gäggeler, H., James, P., Kentarchos, T., Kromp-Kolb, H., Krüger, B., Land, C., Meloen, J., Papayannis, A., Priller, A., Seibert, P., Sprenger, M., Roelofs, G. J., Scheel, H. E., Schnabel, C., Siegmund, P., Tobler, L., Trickl, T., Wernli, H., Wirth, V., Zanis, P., Zerefos, C. (2003). Stratosphere-troposphere exchange: A review, and what we have learned from STACCATO. *Journal of Geophysical Research: Atmospheres, 108*(D12). doi:10.1029/2002JD002490

Turnock, S. T., Allen, R. J., Andrews, M., Bauer, S. E., Deushi, M., Emmons, L., Good, P., Horowitz, L., John, J. G., Michou, M., Nabat, P., Naik, V., Neubauer, D., O'Connor, F. M., Olivié, D., Oshima, N., Schulz, M., Sellar, A., Shim, S., Takemura, T., Tilmes, S., Tsigaridis, K., Wu, T., Zhang, J. (2020). Historical and future changes in air pollutants from CMIP6 models. *Atmos Chem Phys, 20*(23), 14547-14579. doi:10.5194/acp-20-14547-2020

Westervelt, D. M., Ma, C. T., He, M. Z., Fiore, A. M., Kinney, P. L., Kioumourtzoglou, M. A., Wang, S., Xing, J., Ding, D., Correa, G. (2019). Mid-21st century ozone air quality and health burden in China under emissions scenarios and climate change. *Environ Res Lett, 14*(7), 074030. doi:10.1088/1748-9326/ab260b

Young, P. J., Naik, V., Fiore, A. M., Gaudel, A., Guo, J., Lin, M. Y., Neu, J. L., Parrish, D. D., Rieder, H. E., Schnell, J. L., Tilmes, S., Wild, O., Zhang, L., Ziemke, J., Brandt, J., Delcloo, A., Doherty, R. M., Geels, C., Hegglin, M. I., Hu, L., Im, U., Kumar, R., Luhar, A., Murray, L., Plummer, D., Rodriguez, J., Saiz-Lopez, A., Schultz, M. G., Woodhouse, M. T., Zeng, G. (2018). Tropospheric Ozone Assessment Report: Assessment of global-scale model performance for global and regional ozone distributions, variability, and trends. *Elementa: Science of the Anthropocene, 6*, 10. doi:10.1525/elementa.265

Zhang, J., Wei, Y., Fang, Z. (2019). Ozone Pollution: A Major Health Hazard Worldwide. *Frontiers in Immunology, 10*. Retrieved from https://www.frontiersin.org/journals/immunology/articles/10.3389/fimmu.2019.02518

Zhu, L., Jacob, D. J., Keutsch, F. N., Mickley, L. J., Scheffe, R., Strum, M., González Abad, G., Chance, K., Yang, K., Rappenglück, B., Millet, D. B., Baasandorj, M., Jaeglé, L., Shah, V. (2017). Formaldehyde (HCHO) As a Hazardous Air Pollutant: Mapping Surface Air Concentrations from Satellite and Inferring Cancer Risks in the United States. *Environmental Science & Technology, 51*(10), 5650-5657. doi:10.1021/acs.est.7b01356